Biomech Model Mechanobiol (2015) 14:195–215
DOI 10.1007/s10237-014-0607-3

REVIEW

Use it or lose it: multiscale skeletal muscle adaptation to mechanical stimuli

Katrina M. Wisdom · Scott L. Delp · Ellen Kuhl

Received: 19 March 2014 / Accepted: 15 July 2014 / Published online: 9 September 2014

Abstract Skeletal muscle undergoes continuous turnover to adapt to changes in its mechanical environment. Overload increases muscle mass, whereas underload decreases muscle mass. These changes are correlated with, and enabled by, structural alterations across the molecular, subcellular, cellular, tissue, and organ scales. Despite extensive research on muscle adaptation at the individual scales, the interaction of the underlying mechanisms across the scales remains poorly understood. Here, we present a thorough review and a broad classification of multiscale muscle adaptation in response to a variety of mechanical stimuli. From this classification, we suggest that a mathematical model for skeletal muscle adaptation should include the four major stimuli, overstretch, understretch, overload, and underload, and the five key players in skeletal muscle adaptation, myosin heavy chain isoform, serial sarcomere number, parallel sarcomere number, pennation angle, and extracellular matrix composition. Including this information in multiscale computational models of muscle will shape our understanding of the interacting mechanisms of skeletal muscle adaptation across the scales. Ultimately, this will allow us to rationalize the design of exercise and rehabilitation programs, and improve the long-term success of interventional treatment in musculoskeletal disease.

Keywords Skeletal muscle · Growth and remodeling · Adaptation · Lengthening · Thickening

K. M. Wisdom · S. L. Delp · E. Kuhl
Department of Mechanical Engineering,
Stanford University, Stanford, CA 94305, USA

S. L. Delp · E. Kuhl (✉)
Department of Bioengineering, Stanford University,
Stanford, CA 94305, USA
e-mail: ekuhl@stanford.edu

1 Motivation

Skeletal muscle undergoes remarkable adaptations to mechanical stimuli. Weight lifters who regularly generate large muscle forces can nearly double the size of their muscles during their careers (D'Antona et al. 2006). Eccentric exercises enable muscle fiber lengthening (Brockett et al. 2001; Lynn and Morgan 1994). Conversely, individuals who decrease weight bearing on a lower limb experience a decrease in muscle volume (Psatha et al. 2012; Campbell et al. 2013). Chronic high-heel wearers, who keep their calf muscles immobilized at short lengths, develop shorter muscles (Csapo et al. 2010).

Figure 1 illustrates the multiscale architecture of skeletal muscle. Structural changes across the molecular, subcellular, cellular, tissue, and organ scales collectively contribute to macroscopic adaptations in overall muscle structure; on the molecular scale, myosin, the key contractile protein, may switch isoform types, changing the intrinsic speed of force generation (Jürimäe et al. 1996; Goldspink and Scutt 1992; Williamson 2001; De Deyne et al. 1999). On the subcellular scale, in response to elevated forces, more sarcomeres, the force-producing units of muscle, are built and added in parallel, increasing muscle cross-sectional area (Johnson and Klueber 1991; Farup et al. 2012). Conversely, in response to disuse, sarcomeres are lost, decreasing muscle cross-sectional area (Narici and Maganaris 2007; Campbell et al. 2013; Yasuda et al. 2005). In response to chronic overstretch (Boakes et al. 2007; Lindsey et al. 2002) and eccentric exercise (Blazevich et al. 2007; Seynnes et al. 2007a; Lynn and Morgan 1994), sarcomeres are added in series to cause muscle lengthening. Conversely, understretch initiates a decrease in sarcomeres in series and muscle shortening (Csapo et al. 2010; Heslinga et al. 1995b; Tabary et al. 1972; Baker and Matsumoto 1988). On the cellular scale, the chang-

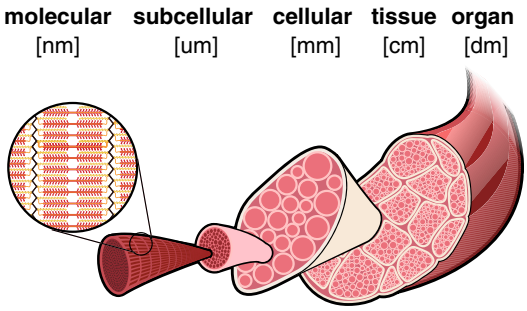

Fig. 1 Length scales of skeletal muscle adaptation. Muscle adaptation to mechanical stimuli spans from the molecular to the organ scale, bridging eight orders of magnitude in length

ing number of contractile units affects active force generation of muscle fibers. On the tissue scale, passive structures may respond to mechanical stimuli through changes in volume and composition, altering the overall tissue stiffnesses (Kjaer 2004; Williams et al. 1998; Tardieu et al. 1982; Hoang et al. 2007). On the organ scale, the organization of muscle fibers, or muscle architecture, may change and contribute to muscle adaptation (Aagaard et al. 2001; Farup et al. 2012; Psatha et al. 2012; Campbell et al. 2013).

The complex process by which muscles adapt to mechanical stimuli spans several length scales (Taber 1995). The past three decades have generated a substantial body of the literature that addresses either different length scales or different mechanical stimuli. Some overviews focus on individual length scales, either molecular (Haddad and Roy 2003; Billeter et al. 1997; Baldwin and Haddad 2001), subcellular (Ehler and Gautel 2008), or cellular (Haddad et al. 2003a; Tidball 2005a; Carson and Wei 2000). Others focus on a single mechanical stimulus, for example, underload through limb suspension (Hackney and Ploutz-Snyder 2012), underload in low-gravity environments (Adams et al. 2003a; Trappe 2002), or overload through resistance training (Roig et al. 2009; Hedayatpour and Falla 2012; Deschenes and Kraemer 2002).

Despite extensive efforts, there are almost no overviews that span multiple length scales and multiple mechanical stimuli. This is the objective of our review. By focusing on how changes across the scales cumulatively result in altered form and function, we aim to bring a unifying perspective to the process of skeletal muscle adaptation. We thoroughly review and classify muscle adaptation processes across the scales and highlight individual and mixed mechanical stimuli. Synthesizing published experimental data, we propose suitable muscle adaptation models and discuss their potential use. In the following, we use the word model to refer to a mathematical model, the algebraic equation to characterize a specific phenomenon.

We acknowledge that hormonal, neural, nutritional, and metabolic factors, as well as age, gender, and species, among other factors, can significantly influence the adaptation of skeletal muscle. For the sake of clarity, we exclude these factors in this review. The tendon also plays a critical role in skeletal muscle adaptation. To focus on muscle tissue alone, we omit the tendon in the following discussion.

In the remainder of this manuscript, we adapt the following terminology: Activated muscle generates force. We specify muscle force as *isometric* if generated by a muscle maintained at constant length, as *concentric* if generated through muscle shortening, and as *eccentric* if generated through muscle lengthening. When the sarcomeres operate at their optimal length, they generate maximum force. Peak isometric muscle stress refers to the maximum isometric muscle force divided the physiological cross sectional area of the whole muscle. Peak isometric fiber stress refers to the maximum isometric fiber force divided by the fiber cross-sectional area.

In what follows, we explore four types of chronic mechanical stimuli that trigger muscle adaptation: *overstretch*, the passive extension of muscle beyond its resting length; *understretch*, the passive shortening of muscle below its resting length; *overload*, the active force generation beyond what is needed to maintain the muscle; and *underload*, the active force generation below what is needed to maintain the muscle.

2 Muscle anatomy and physiology

2.1 Anatomy and physiology on the molecular and subcellular scales

Sarcomeres, approximately 3 μm long assemblies of proteins, are the contractile units of skeletal muscle (Llewellyn et al. 2008; Cromie et al. 2013). Contraction requires activity between two major protein filaments in the sarcomere: thick filaments of myosin and thin filaments of actin (Lieber 2009). According to the sliding filament theory, the interdigitation of these two filaments is the mechanism of force generation (Huxley and Hanson 1954).

Figure 2 illustrates a sarcomere unit as the region between two adjacent Z-disks (Kho et al. 2012). The thick myosin filament is a chain-joining molecule of one isoform of the myosin heavy chain protein. The primary myosin heavy chain isoforms in skeletal muscle are the slow Type I and the fast Type IIa and IIb isoforms. However, because these isoforms can switch, muscles also express intermediate, transitional isoforms (Williamson 2001; Caiozzo 2002). For different myosin heavy chain isoforms, we can model the force–velocity relationship as

$$F_{\text{fib}}^{\text{act}}(\dot{\lambda}) = \frac{\beta}{(0.25 + 0.75\,\alpha)\,\dot{\lambda}^{\max}}\,\dot{\lambda} + \alpha\,\bar{F}\,, \qquad \text{(Fig. 3)}$$

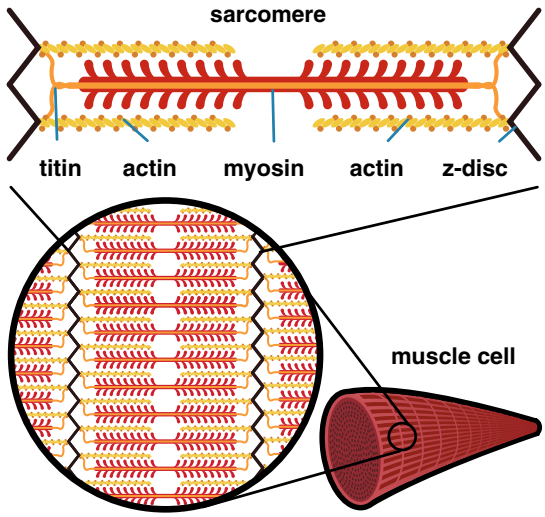

Fig. 2 Anatomy and physiology on the molecular and subcellular scales. The sarcomere is defined as the region between two Z-disks. The Z-disk is connected to myosin via titin. To generate force, myosin filament heads ratchet along actin filaments. The myosin heavy chain isoform influences the intrinsic velocity of active force generation. The titin filament primarily affects the passive fiber force

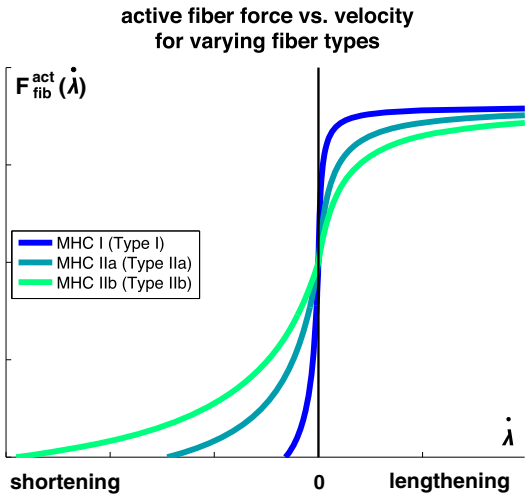

Fig. 3 Active fiber force $F_{\text{fib}}^{\text{act}}$ versus velocity $\dot{\lambda}$ for different myosin heavy chain isoforms. Myosin heavy chain Type I is associated with slow isoforms; myosin heavy chain Types IIa and IIb are associated with fast isoforms

where α is the level of muscle activation, $\dot{\lambda}^{\max}$ is the maximum contraction velocity, and $\bar{F}$ is a force–length scaling factor. To account for the asymmetry between sarcomere shortening and lengthening, the parameter β varies between $\beta = \alpha\bar{F} + 4F$ for shortening with $F \leq \alpha\bar{F}$ and $\beta = 10\,[\alpha\bar{F}F^{\max} - F]/[\bar{F}^{\max} - 1]$ for lengthening with $F > \alpha\bar{F}$ (Thelen 2003).

Figure 3 illustrates how the myosin heavy chain isoform affects the force–velocity relationship of skeletal muscle (Caiozzo 2002). The curves reflect the classic response of the Hill muscle model (Hill 1938; Millard et al. 2013; Thelen 2003), calibrated with human fiber experiments (Bottinelli et al. 1996). The different isoforms interdigitate with actin at different speeds, hence their associations as slow and fast (Scott et al. 2001). Fiber-type distribution is correlated with sensitivity of adaptation to particular stimuli, with slow muscles being sensitive to underload (Thomason and Booth 1990) and fast muscles being sensitive to overload (Gregory et al. 1986; Tesch 1988).

Myosin filaments are connected to Z-disks by a large structural protein called titin (Tskhovrebova et al. 1997). When muscle is stretched, the titin protein resists passive tension (Gautel 2011b; Magid and Law 1985). Titin is the main contributor to the passive force along the fiber direction on the subcellular scale (Gajdosik 2001; Patel and Lieber 1996). We can model the characteristic stretch-stiffening behavior along the fiber direction using a two-component wormlike chain model for the titin protein,

$$F_{\text{fib}}^{\text{pas}}(\lambda) = \frac{k_B T}{A}\left(\frac{1}{4\,(2-\lambda)^2} - \frac{5}{4} + \lambda\right), \qquad \text{(Fig. 4)}$$

where k_B is the Boltzmann constant, T is the absolute temperature, and A is the persistence length (Bustamante et al. 1994; Tskhovrebova et al. 1997). To account for the two major subregions of the titin protein, we can model titin as two wormlike chains in series with individual parameters for each subregion.

Figure 4 illustrates the passive force–stretch response for different titin isoforms. Titin isoforms may vary in length in different muscle types, but also along a single muscle (Granzier et al. 2000). The length of a particular titin subregion is related to the myosin heavy chain isoform; longer subregions are weakly correlated with slow Type I myosin heavy chain isoforms and shorter subregions with fast Type II myosin heavy chain isoforms (Granzier et al. 2000).

In addition to titin, the intermediate filament desmin, the actin and myosin filaments themselves, and the actin–myosin cross-links may contribute to the passive fiber force on the subcellular scale (Wang and Ramirez-Mitchell 1983; Shah et al. 2002; Peters et al. 2003; Gajdosik 2001).

2.2 Anatomy and physiology on the cellular scale

A muscle cell, or muscle fiber, is of cylindrical shape, between 10 µm to 100 µ m in diameter and up to several centimeters in length (Lieber 2009).

Figure 5 illustrates how thousands of myofibrils, or strands of sarcomeres in series, make up a muscle fiber and account for about 80 % of the total muscle fiber volume (Sherwood 2010). The number of sarcomeres in series and in parallel influences the muscle fiber length and cross-sectional area, which, in turn, affect the cell's force-generating ability. To

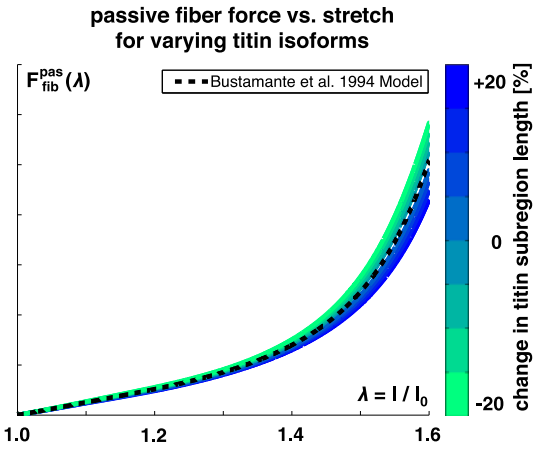

Fig. 4 Passive fiber force $F_{\text{fib}}^{\text{pas}}$ versus fiber stretch λ. The passive force increases exponentially with increasing stretch, reflecting the wormlike chain behavior of titin. Increasing or decreasing the stretch of a titin subregion, shown in *blue* and *green*, increases or decreases the passive force in the fiber direction

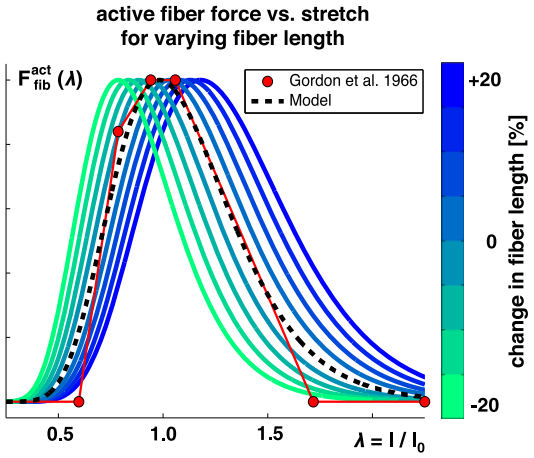

Fig. 6 Active fiber force $F_{\text{fib}}^{\text{act}}$ versus fiber stretch λ. The active force increases toward the optimal fiber length and then decays. Adding or removing sarcomeres in series, shown in *blue* and *green*, increases or decreases the optimal fiber length. Modeled force predicts experimentally measured force shown in *red* (Gordon et al. 1966)

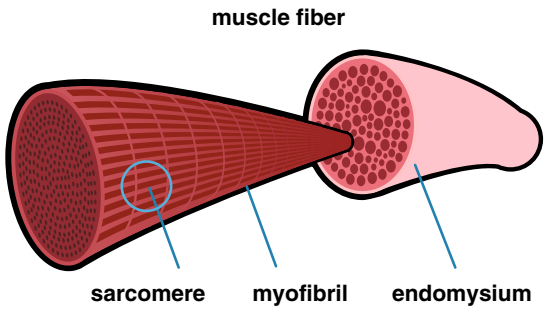

Fig. 5 Anatomy and physiology on the cellular scale. Sarcomeres arranged in series form myofibrils, which, arranged in parallel, make up the muscle cell or muscle fiber. Muscle fibers are surrounded by endomysium

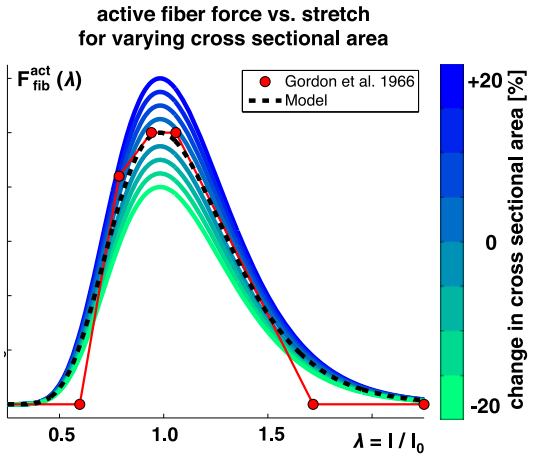

Fig. 7 Active fiber force $F_{\text{fib}}^{\text{act}}$ versus fiber stretch λ. The active force increases toward the optimal fiber length and then decays. Adding or removing sarcomeres in parallel, shown in *blue* and *green*, increases or decreases the fiber cross-sectional area, which increases or decreases the active fiber force. Modeled force predicts experimentally measured force shown in *red* (Gordon et al. 1966)

model the active force–length relationship, we could adapt a phenomenological multi-linear (Gordon et al. 1966) or multi-quadratic (Blemker et al. 2005a) approach. Instead, here, we motivate the active force–length relationship microscopically from actin–myosin bridging using the probability density function of a log-normal distribution,

$$F_{\text{fib}}^{\text{act}}(\lambda) = \frac{1}{\lambda\,\sigma\sqrt{2\pi}}\exp\left(-\frac{(\ln(\lambda)-\lambda_{\text{opt}})^2}{2\,\sigma^2}\right), \quad \text{(Figs. 6, 7)}$$

where the optimal fiber stretch λ_{opt} defines the location of the peak of the curve and the standard deviation σ defines its width.

Figure 6 illustrates the effects of adding and removing sarcomeres in series at constant fiber length, which shift the force–length curve horizontally through scaling the optimal fiber length λ_0. Increasing or decreasing the serial sarcomere number increases or decreases the optimal fiber length at which the maximum force is generated.

Figure 7 illustrates the effects of adding and removing sarcomeres in parallel, which shift the force–length curve vertically through scaling the force F. Increasing or decreasing the parallel sarcomere number increases or decreases the fiber cross sectional area, which increases or decreases the active fiber force.

2.3 Anatomy and physiology on the tissue scale

Skeletal muscle fibers are embedded in the extracellular matrix and arranged in bundles called fascicles (Huijing

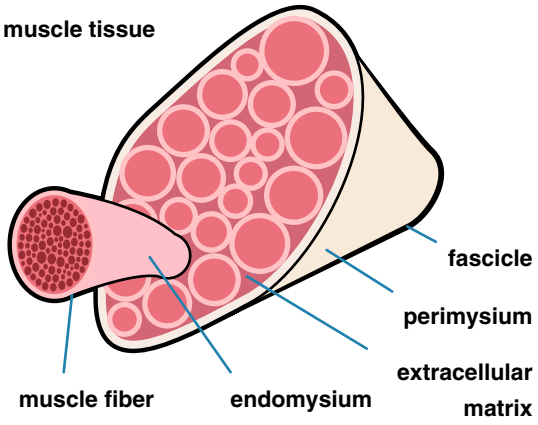

Fig. 8 Anatomy and physiology on the tissue scale. Muscle fibers, embedded in a collagenous extracellular matrix, form a fascicle. Muscle fibers are surrounded by the endomysium, fascicles are surrounded by the perimysium, and the whole muscle is surrounded by epimysium

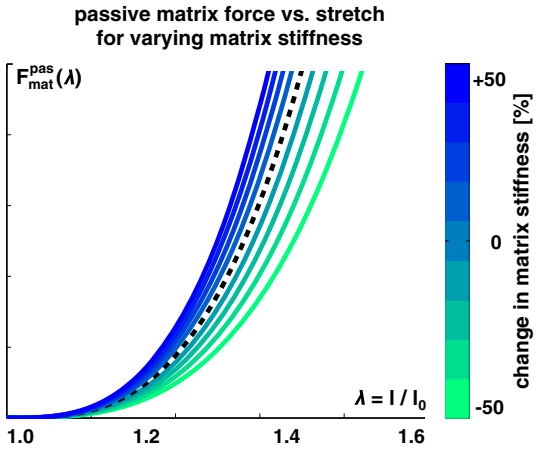

Fig. 9 Passive extracellular matrix force F^{pas}_{mat} versus extracellular matrix tissue stretch λ. The passive force increases exponentially with increasing stretch, reflecting collagen fiber untangling and stiffening. Increasing or decreasing the collagen content increases or decreases the matrix stiffness, shown in *blue* and *green*, and increases or decreases the passive force

1999). The intramuscular connective tissue, which consists primarily of collagen, can account for 1–10 % of the total muscle mass, but may vary widely among different muscle types (Kjaer 2004).

Figure 8 illustrates the key contributors to muscle mechanics on the tissue scale, the extracellular matrix, the endomysium surrounding each muscle fiber, the perimysium surrounding each fascicle, and the epimysium surrounding the whole muscle (Purslow and Trotter 1994). The extracellular matrix contributes significantly to the passive mechanical properties of skeletal muscle (Smith et al. 2011). We can model the passive matrix force using a one-dimensional version of the classic Holzapfel model for soft biological tissue (Holzapfel 2000; Holzapfel et al. 2000), projected onto the collagen fiber direction,

$$F^{pas}_{mat}(\lambda) = c_0\,[\lambda - 1] + \frac{c_1}{2\,c_2}\exp\left(c_2[\lambda - 1]^2\right). \qquad \text{(Fig. 9)}$$

In the general three-dimensional setting, the parameters c_0 and c_1 scale the isotropic and anisotropic behavior and the parameter c_2 characterizes the passive tissue nonlinearity.

Figure 9 illustrates the characteristic passive force–stretch relationship of skeletal muscle. The passive tissue force increases exponentially with increasing stretch, reflecting collagen fiber untangling (Storm et al. 2005) and collagen stiffening (Münster et al. 2013). Increasing or decreasing the collagen content increases or decreases the passive force. As a result, changes in collagen content and collagen microstructure influence the passive resistance of the whole muscle (Huijing 1999; Yucesoy et al. 2003).

2.4 Anatomy and physiology on the organ scale

Whole muscles can be several centimeter up to a few decimeters long. As illustrated in Fig. 10, the cross-sectional area

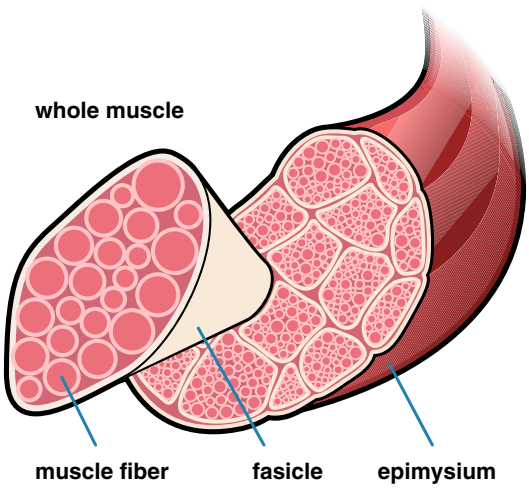

Fig. 10 Anatomy and physiology on the organ scale. A bundle of fascicles are contained within the epimysium, the outermost connective tissue layer, to form the whole muscle

and length of individual muscle fibers, which are closely correlated to the parallel and serial sarcomere numbers, affect the force generating ability of skeletal muscle. Muscle architecture, the three-dimensional arrangement of fibers, affects the mechanical behavior on the organ scale.

A critical organ level measure of muscle architecture is the pennation angle, the angle between muscle fibers and muscle force. The pennation angle varies significantly between different muscles (Schenk et al. 2013); in muscles with a parallel muscle architecture, muscle fibers are aligned with the force-generating axis, the pennation angle is zero, and the characteristic muscle area is the anatomical cross-section area. For muscles with pennate muscle architecture, muscle

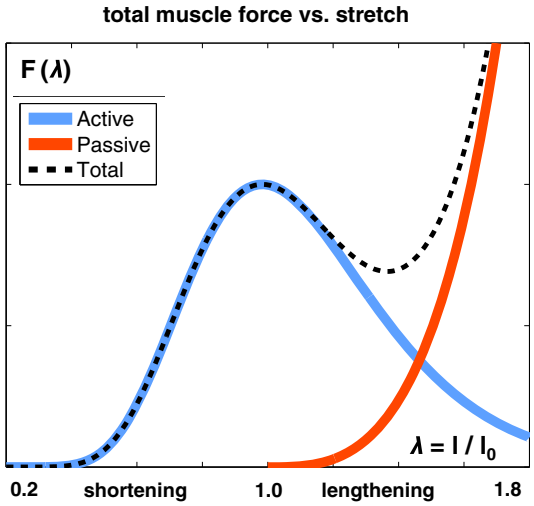

Fig. 11 Total muscle force F versus muscle stretch λ. As the sum of the active and passive forces F_{act} and F_{pas}, the total muscle force peaks and drops in agreement with the active force and then stiffens drastically in agreement with the passive force

fibers are at an angle to the force-generation axis, and the characteristic muscle area is the physiological cross sectional area.

The active force $F_{\text{fib}}^{\text{act}}$ from Figs. 6 and 7, scaled by the active force–velocity relationship in Fig. 3, supplemented by the passive force–length relationships on the cellular and tissue scales $F_{\text{fib}}^{\text{pas}}$ and $F_{\text{mat}}^{\text{pas}}$ in Figs. 4 and 9, collectively characterize skeletal muscle mechanics on the organ scale. Figure 11 illustrates the total muscle force,

$$F(\lambda) = F_{\text{fib}}^{\text{act}} + F_{\text{fib}}^{\text{pas}} + F_{\text{mat}}^{\text{pas}}, \qquad \text{(Fig. 11)}$$

which captures the peak and drop of the active cell force $F_{\text{fib}}^{\text{act}}$ and the drastic stiffening of the passive cellular and extracellular matrix forces $F_{\text{fib}}^{\text{pas}}$ and $F_{\text{mat}}^{\text{pas}}$.

3 Muscle physiology of adaptation

Tables 1, 2, 3, 4 summarizes the literature on multiscale muscle adaptation to various mechanical stimuli in animals and humans. In the following subsections, we discuss these mechanisms in detail.

3.1 Physiology of adaptation on the molecular and subcellular scales

3.1.1 Adaptation of myosin heavy chain isoform

The myosin heavy chain isoform expression in skeletal muscle can change in response to mechanical cues. Muscle remodeling in favor of a greater percentage of slower myosin heavy chain isoforms occurs in animals subjected to stretch, overload, and eccentric exercise (Goldspink and Scutt 1992; Caiozzo 2002; Caiozzo et al. 1997; De Deyne et al. 1999). Animal experiments have also shown that the sarcomeres added in response to overload express primarily the slow myosin heavy chain isoform (Talmadge and Roy 1996).

In humans, myosin heavy chain adaptation is not as well understood. Some studies reported shifts toward slower isoforms in response to sufficient overload (Andersen and Aagaard 2000; Fry 2004; Jürimäe et al. 1996; Williamson 2001), while others found no significant change (Aagaard et al. 2001; Pansarasa et al. 2009). In response to underload, limb unweighting (Andersen and Aagaard 2000), bed rest (Bamman and Clarke 1998; Berg et al. 1997) and microgravity (Zhou et al. 1995; Edgerton et al. 1995) display mixed results. Some studies reported a fractional decrease in slow-twitch fibers and a fractional increase in fast-twitch fibers (Zhou et al. 1995; D'Antona et al. 2003; Andersen and Aagaard 2000; Edgerton et al. 1995), while other studies found no change (Berg et al. 1997; Bamman and Clarke 1998).

Level of neural activation is a major difference among these disuse models. This presents a problem because muscle adaptation can be regulated by neural signals (Kraus et al. 1994; Pette and Staron 2000) and even neural factors unrelated to the activation level (Grossman et al. 1998; Roy et al. 1991). Most studies do not involve completely severing the nervous system connection. This implies that neural activation remains possible, even in complete unloading (Fournier et al. 1983). Several studies have isolated the effect of neural factors with constant levels of disuse and have found more dramatic shifts toward faster myosin heavy chain isoforms in the absence of these signals (Ausoni et al. 1990; Grossman et al. 1998). Approximately 40 % of Type I MHC composition of the adult rat soleus has been attributed to activation-related events, implicating variation in neural factors among disuse experiments as a major contributor to discrepancies in results (Grossman et al. 1998).

3.1.2 Adaptation of titin protein isoform

Despite intense studies, our understanding of how the titin protein may adapt to mechanical stimuli is still incomplete (Neagoe et al. 2003). Underload experiments in rat have reported mixed results; one study has shown that titin isoform size and density decrease (Kasper and Xun 2000), while other studies found decreased density but not length (Toursel et al. 2002) or no change in length or density, but an apparent decrease in elasticity (Goto et al. 2003). Although titin isoform size is weakly correlated to myosin heavy chain type (Prado et al. 2005), the precise effect of titin adaptation on overall muscle function is still under intense debate (Neagoe et al. 2003). It is clear though that titin adaptation has similar

Table 1 Overstretch. Observed adaptation and key literature. ECM = Extracellular Matrix; MHC = Myosin Heavy Chain

Stimulus	Mechanism	Subcellular	Cellular	Tissue	Organ
Overstretch 	Limb lengthening (Boakes et al. 2007; De Deyne 2002; Elsalanty et al. 2007; Lindsey et al. 2002; Makarov et al. 2009; Simpson and Williams 1995; Williams et al. 1998), Immobilization in lengthened position (Tabary et al. 1972; Pontén and Fridén 2008; Williams and Goldspink 1971; Pattullo et al. 1992; Goldspink and Scutt 1992), stretch regimen (Nordez et al. 2009; Gajdosik et al. 2007; Nordez et al. 2006; LaRoche and Connolly 2006; Nakamura et al. 2012; Reid and Mcnair 2004; Goldspink 1999)	Sarcomeres in series ↑ (Makarov et al. 2009; Boakes et al. 2007; Lindsey et al. 2002; Simpson and Williams 1995; Williams and Goldspink 1971; Tabary et al. 1972; De Deyne 2002) Sarcomere length ↑ (Makarov et al. 2009; Elsalanty et al. 2007) Slower MHC ↑ (De Deyne et al. 1999; Goldspink and Scutt 1992)	Fiber length ↑ (Makarov et al. 2009; Elsalanty et al. 2007; Lindsey et al. 2002) Slower fiber type ↑ (Pattullo et al. 1992; De Deyne et al. 1999)	Passive stiffness ↑ (Reid and Mcnair 2004; Williams et al. 1998), mixed (Nordez et al. 2006), NC (LaRoche and Connolly 2006; Gajdosik et al. 2007) ECM ↑ (Pontén and Fridén 2008) Collagen ↑ (Williams et al. 1998)	Pennation angle ↓ (Elsalanty et al. 2007) Fascicle length ↑ (Boakes et al. 2007; Elsalanty et al. 2007; Williams et al. 1998; Simpson and Williams 1995)

Table 2 Understretch. Observed adaptation and key literature. CSA = Cross Sectional Area; ECM = Extracellular Matrix; MHC = Myosin Heavy Chain

Stimulus	Mechanism	Subcellular	Cellular	Tissue	Organ
Understretch 	Immobilization in shortened position (Williams and Goldspink 1978, 1971, 1973; Heslinga et al. 1995b; Csapo et al. 2010; Tabary et al. 1972; Williams and Catanese 1988; Baker and Matsumoto 1988; Williams and Goldspink 1984), Postural misalignment and muscle imbalance (Gossman et al. 1982), tenotomy (Baker and Matsumoto 1988)	Sarcomeres in series ↓ (Tabary et al. 1972; Williams and Goldspink 1978, 1971, 1973; Heslinga et al. 1995b; Csapo et al. 2010; Baker and Matsumoto 1988) Faster MHC ↑ (Goldspink and Scutt 1992)	Fiber CSA ↓ (Heslinga et al. 1995b)	Passive stiffness ↑ (Tabary et al. 1972; Williams and Goldspink 1978; Tardieu et al. 1982) ECM ↑ (Williams and Goldspink 1984)	Fascicle length ↓ (Csapo et al. 2010) Collagen ↑ (Williams and Goldspink 1984)

Table 3 Overload. Observed adaptation and key literature. Anat. = Anatomical; CON = Concentric; CSA = Cross Sectional Area; ECC = Eccentric; MHC = Myosin Heavy Chain; ∗ = inferred from change in ber dimensions

Stimulus	Mechanism	Subcellular	Cellular	Tissue	Organ
Overload 	Functional overload (Fry 2004; Talmadge and Roy 1996; Hubbard et al. 1975; Johnson and Klueber 1991), Resistance exercise (Farup et al. 2012; Moore et al. 2005; Mackey et al. 2011; Erskine et al. 2010a; Kubo et al. 2010; Pansarasa et al. 2009; Blazevich et al. 2007; Seynnes et al. 2007a; Moore et al. 2005; Kraemer et al. 2004a; Shoepe et al. 2003; Williamson 2001; Aagaard et al. 2001; Andersen and Aagaard 2000; Janecki et al. 2011; Brockett et al. 2001; Seger et al. 1998; Jürimäe et al. 1996; Peters et al. 2003; Lynn and Morgan 1994; Kjaer 2004; Yu et al. 2004; Simoneau et al. 1985; Hoang et al. 2007; Miller et al. 2005)	Sarcomeres in series: ↑ (Seynnes et al. (2007a); Blazevich et al. (2007))[a] (Lynn and Morgan 1994; Yu et al. 2004) (ECC), ↓ (Lynn and Morgan 1994) (CON) Sarcomeres in parallel ↑ (Farup et al. 2012; Shoepe et al. 2003; Aagaard et al. 2001; Johnson and Klueber 1991)[a] Slower MHC ↑ (Williamson 2001; Andersen and Aagaard 2000; Jürimäe et al. 1996; Talmadge and Roy 1996; Fry 2004), NC (Aagaard et al. 2001; Pansarasa et al. 2009)	Fiber CSA ↑ (Farup et al. 2012; Shoepe et al. 2003; Aagaard et al. 2001; Johnson and Klueber 1991) Fiber F^{max}/CSA ↑ (Pansarasa et al. 2009) Slower fiber type ↑ (Ianuzzo et al. 1976; Andersen and Aagaard 2000; Simoneau et al. 1985), NC (McDonagh and Davies 1984)	Passive stiffness ↑ (Janecki et al. 2011; Kjaer 2004; Hoang et al. 2007) Collagen ↑ (Kjaer 2004; Miller et al. 2005)	Anat. CSA ↑ (Farup et al. 2012; Moore et al. 2005; Erskine et al. 2010a; Kubo et al. 2010; Blazevich et al. 2007; Seynnes et al. 2007a; Kraemer et al. 2004a; Aagaard et al. 2001; Seger et al. 1998; Johnson and Klueber 1991) Volume ↑ (Erskine et al. 2010a; Aagaard et al. 2001) Pennation angle ↑ (Farup et al. 2012; Erskine et al. 2010a; Blazevich et al. 2007; Seynnes et al. 2007a; Aagaard et al. 2001) Fascicle length ↑ (Blazevich et al. 2007; Seynnes et al. 2007a; Brockett et al. 2001) Anat. F^{max}/CSA ↑ (Erskine et al. 2010a)

effects as extracellular matrix adaptation; it primarily affects the passive force contribution.

3.1.3 Adaptation of serial sarcomere number

Overstretch and understretch of skeletal muscle initiate an increase and decrease, respectively, in the serial sarcomere number (Tabary et al. 1972; Williams and Goldspink 1971; Boakes et al. 2007; Heslinga et al. 1995b; Gossman et al. 1982; Csapo et al. 2010). Figure 6 illustrates the effect of serial sarcomere number adaptation.

Serial sarcomere numbers increase in response to immobilization in a stretched position (Tabary et al. 1972; Williams and Goldspink 1971) and limb lengthening (Boakes et al. 2007; Lindsey et al. 2002; Makarov et al. 2009; Simpson and Williams 1995). It is well accepted that passive stretch beyond a physiological threshold initiates the process of sarcomerogenesis through a series of cellular and molecular events (Caiozzo et al. 2002a). However, the precise sequence of mechanotransduction pathways that triggers serial sarcomere adaptation remains largely unknown (Lieber and Friden 2000). It has been hypothesized that the sarcomere number changes to re-establish the optimal sarcomere length, the length at which maximal force production occurs (Burkholder and Lieber 1998). Sarcomeres are primarily added at myotendinous junctions, although it may be possible for them to be added throughout the length of a muscle fiber (Williams and Goldspink 1971; Caiozzo et al. 2002a).

Increased sarcomere lengths, rather than sarcomere numbers, have been observed in a few studies, indicating that adaptation to the overstretch may have been incomplete or partially unsuccessful (Elsalanty et al. 2007; Makarov et al. 2009). Failure of a muscle to properly adapt to the overstretch it experiences may result in contracture or insufficient muscle length (Makarov et al. 2009). Contracture is one of the most common, and painful, complications of limb-lengthening surgery (Makarov et al. 2009; De Deyne 2002).

Because muscle protein synthesis increases more dramatically in stretched and stimulated muscle than in stretched and unstimulated muscle (Goldspink 1978, 1999), active overstretch triggers serial sarcomere addition to a greater extent than passive overstretch (Seynnes et al. 2007a). In rats, eccen-

Table 4 Underload. Observed adaptation and key literature. Anat. = Anatomical; CSA = Cross Sectional Area; MHC = Myosin Heavy Chain; ∗ = inferred from change in ber dimensions

Stimulus	Mechanism	Subcellular	Cellular	Tissue	Organ
Underload 	Limb unweighting (Campbell et al. 2013; Seynnes et al. 2008; de Boer et al. 2007a; Andersen and Aagaard 2000; Hanson et al. 2012; Ogneva 2010; Deschenes 2001; Allen and Linderman 1997; Canon and Goubel 1995; Widrick et al. 2002; Kasper and Xun 2000; Toursel et al. 2002; Goto et al. 2003; Psatha et al. 2012), bed rest (Berg et al. 2007; Akima et al. 2001; Bamman and Clarke 1998; Berg et al. 1997; Widrick et al. 1997; Narici and Maganaris 2007; Trappe et al. 2004a), Immobilization (Ye et al. 2013; Psatha et al. 2012; Yasuda et al. 2005; Oliveira Milani et al. 2008; D'Antona et al. 2003; Gibson et al. 1987), Microgravity (Fitts et al. 2010; Widrick et al. 1999; Caiozzo et al. 1996; Edgerton et al. 1995)	Sarcomeres in parallel ↓ (Bamman and Clarke 1998; Berg et al. 1997; Yasuda et al. 2005; Fitts et al. 2010; Widrick et al. 1999, 1997; Gibson et al. 1987; Deschenes 2001)[a], (Narici and Maganaris 2007) Faster MHC ↑ (Andersen and Aagaard 2000; Caiozzo et al. 1996; D'Antona et al. 2003; Zhou et al. 1995), NC (Hanson et al. 2012; Bamman and Clarke 1998; Berg et al. 1997) Titin length ↓ (Kasper and Xun 2000), density ↓ (Kasper and Xun 2000; Toursel et al. 2002), elasticity ↓ (Goto et al. 2003)	Fiber CSA ↓ (Bamman and Clarke 1998; Berg et al. 1997; Yasuda et al. 2005; Fitts et al. 2010; Widrick et al. 1999, 1997; Gibson et al. 1987; Deschenes 2001), Slow only (Hanson et al. 2012; Allen and Linderman 1997) Fiber F^{max}/CSA ↓ (Widrick et al. 1999, 2002, 1997; Trappe et al. 2004a; D'Antona et al. 2003; Pansarasa et al. 2009) Faster fiber type ↑ (Canon and Goubel 1995; Caiozzo et al. 1996; D'Antona et al. 2003; Edgerton et al. 1995), NC (Yasuda et al. 2005; Berg et al. 1997; Bamman and Clarke 1998)	Passive stiffness NC (Oliveira Milani et al. 2008)	Anat. CSA ↓ (Campbell et al. 2013; Seynnes et al. 2008; de Boer et al. 2007a; Berg et al. 2007; Akima et al. 2001; Psatha et al. 2012; Yasuda et al. 2005) Volume ↓ (Campbell et al. 2013; Seynnes et al. 2008; Psatha et al. 2012) Pennation angle ↓ (Campbell et al. 2013; Seynnes et al. 2008; de Boer et al. 2007a; Psatha et al. 2012) Fascicle length ↓ (Campbell et al. 2013; Seynnes et al. 2008; de Boer et al. 2007a) Anat. F^{max}/CSA ↓ (Seynnes et al. 2008; Yasuda et al. 2005)

tric exercise triggers serial sarcomere deposition (Lynn and Morgan 1994). In humans, eccentric resistance training also leads to serial sarcomere deposition and enables significant fascicle lengthening (Blazevich et al. 2007; Seynnes et al. 2007a). This increase in muscle length enables increased range of motion. Sarcomerogenesis serves as a major subcellular mechanism to reposition the muscle to its optimal position within the new force-length relationship (Williams and Goldspink 1971, 1973; Burkholder et al. 1994).

In response to chronic understretch, the serial sarcomere number decreases. Various animal studies have demonstrated this effect (Baker and Matsumoto 1988; Heslinga et al. 1995b; Tabary et al. 1972; Williams and Goldspink 1971, 1973, 1978). Humans who experience partial or total muscle immobilization (Gossman et al. 1982), for example, by frequently wearing high heels (Csapo et al. 2010), may experience chronic muscle shortening caused by a decrease in sarcomeres in series.

3.1.4 Adaptation of parallel sarcomere number

We commonly assume that cross-sectional area is directly correlated to the number of sarcomeres in parallel (Narici and Maganaris 2007; Potier et al. 2009a; Lieber and Friden 2000; Wickiewicz and Roy 1983). With the exceptions of steroid-induced hypertrophy (MacDougall et al. 1982) or blockage of the transforming growth factor-β family member myostatin (Lee and McPherron 2001), this implies that an increase in cross-sectional area of skeletal muscle fibers indicates the addition of sarcomeres in parallel. An array of studies measure increases or decreases in fiber cross-sectional area, and these results are taken as evidence of parallel sarcomere addition or resorption. In particular, functional overload through targeted muscle removal in animals, e.g., synergist removal (Johnson and Klueber 1991) or surgical ablation, and through resistance exercise (Farup et al. 2012; Aagaard et al. 2001; Shoepe et al. 2003) trigger parallel sarcomere deposition. By

contrast, disuse initiates parallel sarcomere removal (Narici and Maganaris 2007).

3.2 Physiology of adaptation on the cellular scale

3.2.1 Adaptation of cross-sectional area

Increase in fiber cross-sectional area, or fiber hypertrophy, is correlated to the number of sarcomeres added in parallel. Figure 7 illustrates the effect of fiber cross-sectional area adaptation. Chronic overloading in animals initiates an increase in fiber cross-sectional area (Johnson and Klueber 1991). This effect has been recently confirmed in humans in response to resistance exercise (Aagaard et al. 2001; Farup et al. 2012; Shoepe et al. 2003). The observation that protein synthesis increases in response to resistance exercise supports the hypothesis that the increase in cross section reflects an increase in contractile material, and thus in force-generating ability, as illustrated in Fig. 7 (Hubbard et al. 1975; Moore et al. 2005). The increase in satellite cells following resistance exercise may provide the machinery for increased manufacturing of this contractile material (Mackey et al. 2011). Recent studies have emphasized the role of miRNAs in mediating the response and adaptation of skeletal muscle to various modes of exercise (Kirby and McCarthy 2013). Underload initiates a decrease in fiber cross-sectional area, but results vary by disuse model. Some studies of bed rest (Berg et al. 1997; Bamman and Clarke 1998; Widrick et al. 1997), spaceflight (Fitts et al. 2010; Widrick et al. 1999), immobilization in humans (Yasuda et al. 2005; Gibson et al. 1987), and hindlimb suspension in animals (Deschenes 2001) have seen decrease in cross-sectional area across all fiber types. Other animal hindlimb suspension models have shown pronounced atrophy only in slow-twitch fibers (Allen and Linderman 1997; Hanson et al. 2012). Animal age appears to influence the adaptive response of the fiber cross-sectional area (Deschenes 2001); fibers in aged animals may experience delayed atrophy (Yokogawa et al. 2008).

The unclear extent to which neural activation is inhibited may prevent direct comparison among unloading studies (Widrick et al. 2002). Rat experiments on inactivity with and without spinal cord separation have shown that activation-related events account for at least 75 % of the decrease in fiber size (Grossman et al. 1998).

Homeostatic cross-sectional area results from balanced protein synthesis and protein breakdown. Studies indicate that the primary contributor to disuse atrophy is a decrease in protein synthesis rather than an increase in protein breakdown. This imbalance causes a net loss of protein mass and cross-sectional area of individual muscle fibers (Gibson et al. 1987). Both decreased signaling for protein synthesis (decreased demand) or decreased number of satellite cells following atrophy (decreased supply of protein synthesis machinery) may contribute to the atrophy (Allen et al. 1999).

3.2.2 Adaptation of peak isometric fiber stress

Peak isometric fiber stress may change in response to mechanical stimuli. Muscle adaptation to long-duration resistance training can initiate an increase in peak isometric fiber stress (Pansarasa et al. 2009). By contrast, underload induced by limb unweighting (Widrick et al. 2002), immobilization (D'Antona et al. 2003), bed rest (Widrick et al. 1997; Trappe et al. 2004a), and microgravity (Widrick et al. 1999) initiates a decrease. In one study, the decrease in peak isometric fiber stress linearly correlated with the decrease in myosin concentration following underload (D'Antona et al. 2003). Declines in the number of actin–myosin cross-bridges per fiber (D'Antona et al. 2003; Widrick et al. 1999) and in strength per cross-bridge following disuse (Caiozzo 2002) contribute to the loss in muscle strength in response to underload (de Boer et al. 2007a). Further research is needed to identify other contributors to specific tension of the muscle fiber and quantify their importance and plasticity.

3.2.3 Adaptation of fiber type

Delineating muscle fiber types by myosin heavy chain isoform expression profile is most common, although fiber types exhibit differences in metabolic rates, oxidative properties, and isoform expression of other sarcomeric proteins (Pette and Staron 2000). The changes in myosin heavy chain isoform on the molecular scale, alongside these other factors, allow for whole fiber-type transitions in response to mechanical stimuli.

Functional overload (Ianuzzo et al. 1976) and overstretch (Pattullo et al. 1992; De Deyne et al. 1999) are potent initiators of transition to slow-twitch fiber types in animal muscle. Similarly, slow-to-fast fiber-type transitions occur in animals subjected to underload (Canon and Goubel 1995; Caiozzo et al. 1996). Generally, fast fiber types respond more drastically to overload and overstretch, and slow fiber types respond more drastically underload induced changes (Pette and Staron 2000; Widrick et al. 2002).

In humans, fiber-type transitions, especially in response to underload, are less consistent than in animals (D'Antona et al. 2003; Edgerton et al. 1995; Berg et al. 1997; Bamman and Clarke 1998; Yasuda et al. 2005; McDonagh and Davies 1984; Simoneau et al. 1985; Andersen and Aagaard 2000). Mixed stimuli, variations in neural activity, and different methods of fiber-type classification may obfuscate results in adaptive human fiber-type transitions (Pette and Staron 2000). Some experimental stimuli may be insufficient, whereas a three month regimen of heavy-load resistance training successfully initiates transitions to slower fiber

types (Andersen and Aagaard 2000; Simoneau et al. 1985). Elite, high-endurance athletes such as long-distance runners have high percentages of slow fibers (Ricoy et al. 1998), and sprinters and power-weight lifters, who require speed over endurance, have high percentages of fast fibers (Ricoy et al. 1998), which seem to support the "sufficient stimulus" hypothesis. However, genetics may partially explain endowment of fiber types (Baldwin and Haddad 2001; McDonagh and Davies 1984; Komi and Karlsson 1979). Despite extensive research, quantitative characterization of the conditions under which fiber-type transitions definitively occur in humans is still lacking.

Fiber-type adaptation affects both force-generating capacity and sensitivity to future adaptation. Although some studies have noted differences in peak isometric force among fast- and slow-twitch fibers (Mutungi and Ranatunga 1996; Taber 1995; Kovanen et al. 1987), differences in the force–velocity relationship among these fibers, illustrated in Fig. 3, contribute to larger force discrepancies, particularly at high shortening and lengthening velocities. Even so, fiber-type percentage has a smaller effect on whole muscle force, in comparison to other parameters, such as muscle length, cross sectional area, and pennation angle, as long as velocity of contraction does not approach maximum shortening or lengthening (Fig. 3) (Burkholder et al. 1994; Lieber 2009). Predominantly, slow-twitch muscles are more responsive to underload (Thomason and Booth 1990) and that fast-twitch muscles are more sensitive to overload (Gregory et al. 1986; Tesch 1988). Switching myosin heavy chain isoforms and fiber types may thus incrementally alter a muscle's sensitivity to further adaptation.

3.3 Physiology of adaptation on the tissue scale

3.3.1 Adaptation of extracellular matrix volume

Extracellular matrix, through volume, structure, and stiffness variation, adapts in response to mechanical stimuli (Kjaer 2004; Miller et al. 2005). Figure 9 illustrates the effect of extracellular matrix stiffening on the passive force–length properties of skeletal muscle.

Chronic overload, overstretch, and understretch all initiate an increase in the passive stiffness of skeletal muscle (Reid and Mcnair 2004; Williams et al. 1998; Tabary et al. 1972; Williams and Goldspink 1978; Tardieu et al. 1982; Janecki et al. 2011; Kjaer 2004; Hoang et al. 2007). Increased passive stiffness can be facilitated through increased extracellular matrix volume (Pontén and Fridén 2008; Williams and Goldspink 1984), especially that which is enabled by increased collagen content (Williams et al. 1998; Kjaer 2004; Miller et al. 2005). Because collagen is so stiff in comparison to skeletal muscle fibers, a change in collagen content can noticeably alter the passive mechanical properties of skeletal muscle (Kovanen et al. 1987). Further increase in tissue stiffness can arise through reorientation of collagen fibers (Williams and Goldspink 1984). In animal models, changes in extracellular matrix chemistry and fiber cross-linking also alter its passive stiffness (Ahtikoski et al. 2001; Akeson et al. 1977; Woo et al. 1975). Several different mechanisms operate in the regulation of extracellular matrix properties.

Stretch regimens show inconsistent results. This may be because tendon compliance changes in response to mechanical stimuli in conjunction with, or instead of, skeletal muscle passive stiffness (LaRoche and Connolly 2006; Nordez et al. 2006; Kjaer 2004). Passive muscle stiffness is different from range of motion, which is improved through stretching and is associated with improved tendon compliance rather than decreased passive muscle stiffness (Kubo and Kanehisa 2001; Magnusson et al. 2008).

Many questions remain unanswered regarding the underlying mechanisms of extracellular matrix remodeling (Röhrle et al. 2012). However, it is clear that this adaptation contributes significantly to changes of whole muscle properties. Increased stiffness increases load resistance and renders connective tissue more damage resistant, particularly within a remodeling muscle (Kjaer 2004). Increased extracellular matrix may be a temporary response to the injury induced by extreme mechanical stimuli (Gillies and Lieber 2011; Hoang et al. 2007). Extracellular matrix turnover in general facilitates cell migration, formation of new muscle, and reorganization of the extracellular matrix, events necessary for muscle adaptation (Gillies and Lieber 2011). Accumulation or depletion of connective tissue in skeletal muscle may further enable adjustment of the relative importance of the titin protein (Fig. 4) and extracellular matrix material (Fig. 9) to passive properties of skeletal muscle as a whole (Fig. 11) (Neagoe et al. 2003).

3.4 Physiology of adaptation on the organ scale

The consequences of adaptation to mechanical stimuli on the smaller scales collectively contribute to changes on the whole muscle scale.

3.4.1 Adaptation of anatomical cross-sectional area and volume

Overload induced by resistance exercise leads to increased anatomical cross-sectional area (Farup et al. 2012; Moore et al. 2005; Erskine et al. 2010a; Kubo et al. 2010; Blazevich et al. 2007; Seynnes et al. 2007a; Kraemer et al. 2004a; Aagaard et al. 2001; Seger et al. 1998; Johnson and Klueber 1991) and whole muscle volume (Erskine et al. 2010a; Aagaard et al. 2001) in both humans and animals. Sub-

jects in eccentric and concentric training studies experience a greater increase in muscle mass in response to high-intensity eccentric training than in response to concentric training (Roig et al. 2009). This motivated the hypothesis that the higher absolute loads generated during eccentric contractions are the critically important mechanical stimuli (Roig et al. 2009; Booth and Thomason 1991). Controlled animal studies have revealed that intermittent passive stretch may trigger both radial and longitudinal growth (Goldspink 1999). However, this observation may be the result of passive stretch in the presence of rapid natural growth experienced by small rodents (McDonagh and Davies 1984). In humans, passive stretch does not induce significant protein synthesis or hypertrophy (Fowles et al. 2000). What initiates hypertrophy is not well understood; competing hypotheses suggest that either active strain (Fowles et al. 2000) or fiber stress (Goldspink and Yang 2001) may regulate anatomical cross-sectional area.

Underload initiated by disuse causes a drastic decrease in anatomical cross-sectional area (Campbell et al. 2013; Seynnes et al. 2008; de Boer et al. 2007a; Berg et al. 2007; Akima et al. 2001; Psatha et al. 2012; Yasuda et al. 2005) and whole muscle volume (Campbell et al. 2013; Seynnes et al. 2008; Psatha et al. 2012). Two months of disuse can cause a muscle to atrophy to half of its normal size (Sandler 1986). Limited literature is available on the effect of understretch with continued muscle loading, although this situation is commonly experienced in humans by chronic high-heel wearers (Csapo et al. 2010). Although muscles in chronic high-heel wearers shorten, the cross-sectional area of these muscles does not significantly change (Csapo et al. 2010).

Increase and decrease in fiber cross-sectional area translate directly into increase and decrease in anatomical cross-sectional area via the pennation angle.

3.4.2 Adaptation of pennation angle

Pennation angle can vary among different muscles and is highly plastic (Lieber and Friden 2000). Muscle adaptation can include a reorientation of muscle fibers in addition to changes in fiber geometry. Fiber reorientation may affect both the amount of force that can be exerted over a cross-sectional area and the transmission of force among the individual fibers (Seynnes et al. 2007a; Kawakami 1993).

Increased pennation angle is positively correlated with increased sarcomeres in parallel, is negatively correlated with the number of sarcomeres in series, and can change with muscle hypertrophy (Farup et al. 2012; Erskine et al. 2010a; Blazevich et al. 2007; Seynnes et al. 2007a; Aagaard et al. 2001). These observations motivate the hypothesis that the fascicle angle adapts to accommodate hypertrophy within the limited space available in the whole muscle (Kawakami 1993; Blazevich et al. 2007; Aagaard et al. 2001). For a muscle of constant fascicle length, fiber length, and fiber number, experimental evidence indicates that an increase in fiber diameter is correlated to an increase in pennation angle (Kawakami et al. 1995; Maxwell et al. 1974). This fiber-packing strategy allows for maximizing the number of contractile elements attached to a tendon (Kawakami et al. 1995; Burkholder et al. 1994). As expected, an underload induced decrease in anatomical cross-sectional area results in a decrease in pennation angle (Campbell et al. 2013; Seynnes et al. 2008; de Boer et al. 2007a; Psatha et al. 2012).

3.4.3 Adaptation of fascicle length

Eccentric exercise initiates fascicle lengthening (Blazevich et al. 2007; Seynnes et al. 2007a; Brockett et al. 2001), whereas understretch, e.g., in chronic high-heel wearing, initiates fascicle shortening (Csapo et al. 2010). The extent to which the lengthening or shortening of myofibrils, i.e., the addition or resorption of sarcomeres in series, contributes to the change in fascicle length depends on the pennation angle.

The relationships between fascicle length and pennation angle and between pennation angle and anatomical cross-sectional area indicate that whole muscle adaptation is simultaneously dependent on both muscle length and cross-sectional area. For example, in the presence of underload and understretch, e.g., during immobilization in a shortened position, rat muscle cross-sectional area decreases (Heslinga et al. 1995b). A controlled animal model has shown that in the highly pennated gastrocnemius, cross-sectional area changes alone proved sufficient to establish a new muscle force–length relationship without the removal of sarcomeres in series (Heslinga et al. 1995b). In the unipennate soleus, however, cross-sectional area changes alone were insufficient to induce the required change in length, and a removal of sarcomeres in series was necessary. These studies affirm the crucial role of architectural remodeling in skeletal muscle adaptation.

3.4.4 Adaptation of peak isometric muscle stress

Overload increases peak isometric muscle stress (Erskine et al. 2010a), whereas limb unweighting (Seynnes et al. 2008) and immobilization (Yasuda et al. 2005) decrease peak isometric muscle stress. Adaptation to peak isometric fiber stress likely scales up to the organ scale (Pansarasa et al. 2009; D'Antona et al. 2003; Trappe et al. 2004a).

4 Modeling muscle adaptation

The past two decades have seen significant advancements in skeletal muscle modeling. Global, three-dimensional models of electrical activation and mechanical contraction now provide great insight into muscle anatomy, structure, and function on multiple scales (Blemker and Delp 2005; Böl and Reese 2008a; Böl 2010; Röhrle et al. 2008; Röhrle 2010; Oomens et al. 2003; Lemos et al. 2004). Local models complement this insight by studying the interaction among the biochemistry, metabolism, and force production in skeletal muscle (Dash et al. 2007; Murtada et al. 2012). However, muscle models that reliably predict the long-term response of skeletal muscle are still surprisingly rare (Taber 1998; Kuhl 2014). A recent study focused on modeling the adaptation of skeletal muscle in response to chronic understretch and overstretch (Wren 2003). This pioneering work provided valuable insight, but was limited to a one-dimensional model.

First attempts to simulate the chronic adaptation of skeletal muscle in a fully three-dimensional setting using a multiscale, multifield model are currently underway (Zöllner et al. 2012b). These models rely on a three-step procedure: First, they project global, whole muscle strain and stress onto local subcellular stretch and force using microstructural information such as volume fractions and pennation angles. Second, they locally evaluate the biochemistry and metabolism on the cellular scale, for example, by simulating the deposition or removal of sarcomeres in series or in parallel to predict the resulting stretch and force. Third, they recollect this information and translate local cellular stretch and force back to global, whole muscle strain and stress using microstructural information (Göktepe et al. 2010). Key to this method is the modularity of the second step, which enables the seamless integration of various cellular and molecular processes into a whole muscle model (Böl et al. 2013). Finite element methods are typically the first choice to naturally embed this approach by modeling the whole muscle and tissue information globally at the node point level and integrating the cellular and molecular processes locally at the integration point level (Ambrosi et al. 2011; Göktepe et al. 2010a). In the following subsections, we suggest possible muscle adaptation models in response to chronic overstretch, overload, and underload and compare them against experimental and clinical data.

4.1 Modeling adaptation to overstretch

To model skeletal muscle adaptation in response to chronic overstretch, we consult experiments of chronic limb lengthening (Matano et al. 1994). In these experiments, the serial sarcomere number increased exponentially and then converged toward a homeostatic equilibrium value, which was correlated to the amount of overstretch. This motivates the following equation for changes in serial sarcomere number in response to overstretch (Zöllner et al. 2012b),

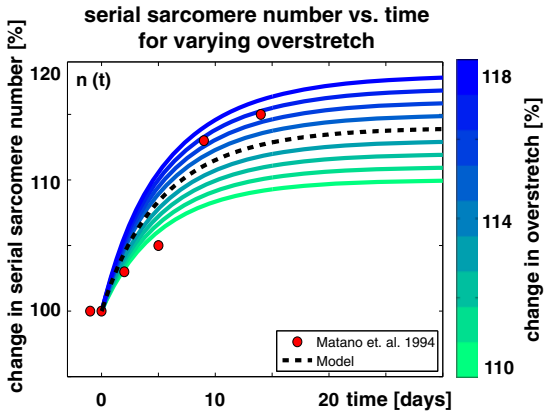

Fig. 12 Serial sarcomere number versus time. The serial sarcomere number increases exponentially and converges toward a homeostatic equilibrium, which depends on the applied overstretch. Increasing or decreasing the overstretch, shown in *blue* and *green*, increases or decreases the serial sarcomere number. Modeled sarcomere numbers, shown as *black dashed line*, show the same trend as experimentally measured sarcomere numbers, shown as *red circles* (Matano et al. 1994)

$$\dot{n}(t) = \frac{1}{\tau}\left(\frac{n^{\max} - n}{n^{\max} - 1}\right)^{\gamma} \left(\lambda^{\mathrm{e}} - \lambda^{\mathrm{o}}\right) . \qquad \text{(Fig. 12)}$$

Here, n is the serial sarcomere number, $n^{\max}$ is its limiting value, τ is a time constant that controls the adaptation speed, and γ controls the nonlinearity of the adaptation process. The switch factor $(\lambda^{\mathrm{e}} - \lambda^{\mathrm{o}})$ controls the amount of overstretch and activates the serial addition of sarcomeres only if the elastic muscle stretch λ^{e} exceeds the physiological baseline value λ^{o}.

Figure 12 illustrates the gradual increase in serial sarcomere number in response to long-term overstretch. On the subcellular scale, the sarcomere number increases gradually to reduce the sarcomere stretch λ^{e} and to reposition the sarcomere and the muscle fiber back into their optimal operating regime (Arnold and Delp 2011). On the organ scale, the muscle increases in length to compensate for the amount of overstretch or passive force (Taber 1998). Increasing or decreasing the amount of overstretch increases or decreases the serial sarcomere number. The model, shown as black dashed line, captures the general trend observed during chronic limb-lengthening experiments in rabbits, shown as red circles, where the serial sarcomere number increased by 14 % to compensate for the chronically applied overstretch of $\lambda = 1.14$ (Matano et al. 1994).

4.2 Modeling adaptation to overload

To model skeletal muscle adaptation in response to chronic overload, we examine results of training protocols, in which

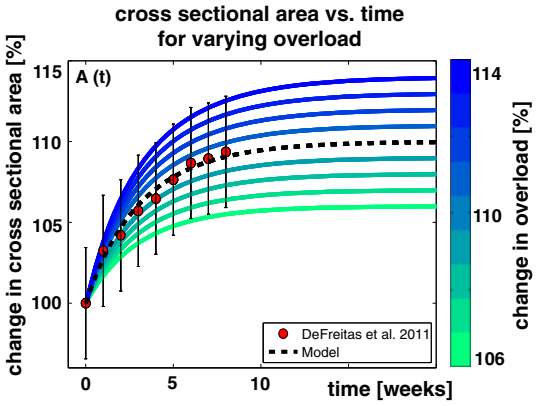

Fig. 13 Cross-sectional area versus time. The cross-sectional area increases exponentially and converges toward a homeostatic equilibrium, which depends on the applied overload. Increasing or decreasing the overload, shown in *blue* and *green*, increases or decreases the cross-sectional area. Modeled cross-sectional areas, shown as *black dashed line*, predict experimentally measured cross-sectional areas, shown as *red circles* (DeFreitas et al. 2011)

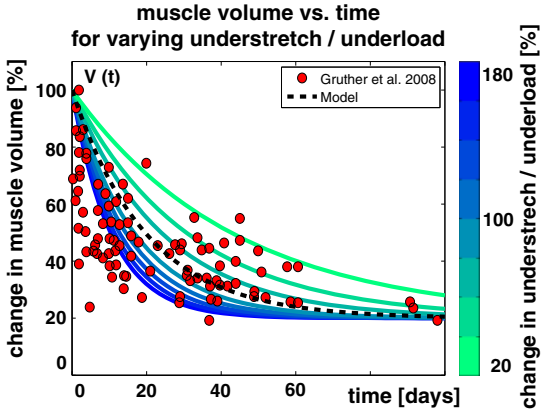

Fig. 14 Muscle volume versus time. The muscle volume decreases exponentially and converges toward a homeostatic equilibrium. The speed of muscle loss depends on the degree disuse or underload. Increasing or decreasing the underload, shown in *blue* and *green*, increases or decreases the speed of muscle loss. Modeled muscle loss, shown as *black dashed line*, shows the same trend as experimentally measured muscle loss, shown as *red circles* (Gruther et al. 2008)

the muscle cross-sectional area of the human thigh was measured throughout a period of 8 weeks of training (DeFreitas et al. 2011). In these experiments, the cross-sectional area increased exponentially and then converged toward a homeostatic equilibrium value. In analogy to the previous section, we can introduce the following equation for changes in cross-sectional area in response to chronic overload (Rausch et al. 2011),

$$\dot{A}(t) = \frac{1}{\tau}\left(\frac{A^{\max} - A}{A^{\max} - 1}\right)^{\gamma}\left(F - F^{\mathrm{o}}\right) . \qquad \text{(Fig. 13)}$$

Here, A is the cross-sectional area, $A^{\max}$ is its limiting value, τ is a time-constant that controls the adaptation speed, and γ controls the nonlinearity of the adaptation process. Conceptually similar to overstretch, we have introduced a switch factor $(F - F^{\mathrm{o}})$ to control the amount of overload. It activates the parallel addition of sarcomeres only if the total muscle force F exceeds the physiological baseline value F^{o}.

Figure 13 illustrates the gradual increase in cross-sectional area in response to long-term training. On the organ scale, the muscle increases its cross-sectional area to compensate for the amount of overload or active force (Taber 1998). On the subcellular scale, these changes are brought about by the parallel addition of sarcomeres, which form additional myofibrils to increase the overall cross-sectional area. Increasing or decreasing the overload increases or decreases the cross-sectional area. The model, shown as black dashed line, agrees well with exercise protocols in humans, shown as red circles, where the cross-sectional area of the right thigh muscles increased by 9.59 %, from 145 to 158.9 cm^2, in response to overload generated by exercise (DeFreitas et al. 2011).

4.3 Modeling adaptation to understrech or underload

To model skeletal muscle adaptation in response to chronic understretch or underload, we consult measurements of patients of the intensive care unit who underwent bed rest over periods of up to 100 days (Gruther et al. 2008). In these patients, the muscle layer thickness decreased exponentially and then converged toward a minimum baseline value. This motivates the following exponential equation for muscle loss in response to chronic understretch or underload,

$$\dot{V}(t) = -\frac{1}{\tau}\left(1 - V^{\min}\right)\exp(-t/\tau) . \qquad \text{(Fig. 14)}$$

Here, V is the normalized muscle volume, and $V^{\min}$ is its minimum baseline value. The time parameter τ, which controls the adaptation speed, can either have a constant value or be a function of the amount of understretch $\tau(\lambda)$ or underload $\tau(F)$. The exponential nature of the muscle loss equation enables its explicit integration to obtain the following direct expression for the whole muscle volume as a function of time, $V(t) = \left(1 - V^{\min}\right)\exp(-t/\tau))$.

Figure 14 illustrates the gradual loss of muscle volume in response to long-term bed rest. On the organ scale, muscle decreases its volume and mass to compensate for the amount of underload. On the subcellular scale, understretch and underload initiate the serial and parallel removal of sarcomeres. Increasing or decreasing the amount of understretch λ or underload F increases or decreases the speed of muscle volume loss τ as shown in blue and green. This model, shown as black dashed line, captures the trend of the skeletal muscle loss in bedridden hospital patients, shown as red circles (Gruther et al. 2008). Using an exponentially decaying

function to model muscle loss as a function of disuse time is supported by prior work, in which an exponential function was utilized to model fiber volume, obtained by biopsy, as a function of time of immobilization (Gibson et al. 1987). In this prior study, fiber volume loss was proportional to loss in protein mass(Gibson et al. 1987). This illustrates that muscle atrophy propagates across the scales, from protein mass via fiber volume to whole muscle volume. These phenomena support the use of exponential multiscale models to characterize muscle loss in response to understretch or underload.

5 Discussion

In this review, we have discussed current challenges in modeling skeletal muscle adaptation. The major roadblock toward reliable, predictive modeling of muscle adaptation is the lack of adequate experimental data with sufficient resolution in both space and time. Most existing datasets on skeletal muscle adaptation report information of a single spatial scale. To truly link cause and effect, it would be critical to characterize the adaptation process across multiple spatial scales. In addition, almost all existing studies are limited to only two time points, the initiation of the adaptation process at time zero and the result at a later time point. To create mathematical models that reliably predict the progression of the muscle adaptation, it would be important to characterize the adaptation process at multiple points in time.

After our thorough literature review, we suggest the following set of experiments to provide insight into the time line of chronic muscle adaptation: (i) monitoring the serial sarcomere number, fiber length, and whole muscle length upon progressive overstretch at multiple time points (Matano et al. 1994) similar to Fig. 12, but now by gradually increasing the magnitude of stretch; (ii) monitoring the parallel sarcomere number, fiber cross sectional area, and anatomical cross-sectional area at multiple time points (DeFreitas et al. 2011) similar to Fig. 13, but now by gradually increasing the magnitude of load; and (iii) monitoring the total sarcomere number, fiber size, and muscle volume upon understretch and underload at multiple time points (Gruther et al. 2008) similar to Fig. 14. On the subcellular scale, recent developments in microendoscopy now enable noninvasive sarcomere imaging both in animals and humans, to characterize changes in serial and parallel sarcomere number in vivo (Llewellyn et al. 2008; Cromie et al. 2013). On the cellular, tissue, and organ scales, features such as fascicle length, pennation angle, and muscle thickness can be characterized noninvasively in vivo using ultrasound (Asakawa et al. 2002).

The measured datasets could then be collectively integrated into a unified, holistic multiscale model of chronic muscle adaptation, which should at least include the following information: (i) at the molecular and subcellular scales: changes in myosin heavy chain isoform, which affect active muscle velocity according to Fig. 3; (ii) at the cellular scale: changes in serial sarcomere number, which affect fascicle length and active muscle force according to Fig. 6; (iii) at the cellular scale: changes in parallel sarcomere number, which affect anatomical cross-sectional area and active muscle force according to Fig. 7; (iv) at the tissue scale: changes in extracellular matrix volume, structure, and composition, which affect passive muscle stiffness according to Fig. 9; (v) at the organ scale: changes in pennation angle, which affect anatomical cross-sectional area and active muscle force. Taken together, these changes in myosin heavy chain isoform, fiber length, fiber cross-sectional area, extracellular matrix stiffness, and pennation angle collectively impair the adaptation of overall muscle form and function.

A model like this includes five key players in chronic muscle adaptation to mechanical stimuli, but it is, of course, not comprehensive. The following information could be included in a more advanced model of chronic muscle adaptation: (vi) at the molecular scale: changes in titin isoform (Kasper and Xun 2000; Toursel et al. 2002; Goto et al. 2003); (vii) at the subcellular scale: changes in number (D'Antona et al. 2003; Widrick et al. 1999) and force (Caiozzo 2002) of actomyosin cross-bridges within the sarcomeres; (viii) at the cellular scale: changes in desmin protein content, as desmin also affects passive myofibril stiffness (Wang and Ramirez-Mitchell 1983; Shah et al. 2002; Peters et al. 2003); (ix) at the organ scale: changes in collagen fiber orientation and extracellular matrix composition (Kuhl and Holzapfel 2007; Saez et al. 2013); (ix) at the organ scale: changes in tendon geometry and tendon stiffness, which affect passive mechanical properties of the muscle-tendon unit (Delp and Zajac 1992). Beyond the organ scale, this approach does not yet address the wide variety of factors that influence muscle adaptation at larger, more integrative scales. This includes muscle-specific architecture, attachment geometry, and function (Blemker and Delp 2006), as well as subject-specific neural factors, age, gender, species, nutrition, and hormone levels (Joo et al. 2013). These factors may significantly affect adaptation (Reeves et al. 2009; Yasuda et al. 2005; Eriksson et al. 2005; Deschenes 2001).

The major advantage of multiscale modeling, in comparison to individual single-scale modeling, is that it will provide a more holistic understanding of skeletal muscle adaptation. Ultimately, multiscale models have the potential to explain mechanisms using parameters that have a clear physical interpretation, rather than using phenomenological parameters that are based on data fitting. For example, multiscale modeling could provide useful bounds on the speed of muscle growth or identify the energy required to build a specific amount of new muscle using assembly kinetics from the molecular and subcellular scales.

6 Conclusion

This review has systematically categorized skeletal muscle adaptation in response to various mechanical stimuli from the molecular to the organ scale. From this classification, we have identified four major driving mechanisms of skeletal muscle adaptation: overstretch, understretch, overload, and underload; and five key players in skeletal muscle adaptation: changes in myosin heavy chain isoform, serial sarcomere number, parallel sarcomere number, pennation angle, and extracellular matrix composition. We have highlighted major dependencies among these variables and the initiators of changes within them. We have discussed the adaptation with respect to isolated and combined mechanical stimuli and reviewed protocols to study their impact in animal models and in human health, training, and rehabilitation. From the insight gained through these studies, we have suggested three muscle adaptation models in response to overstretch, overload, and underload. Mathematical modeling has a tremendous potential in understanding skeletal muscle adaptation across the scales. Computational modeling can naturally integrate the mechanobiology of muscle adaptation at the molecular, subcellular, and cellular scales into the biomechanics at the organ and tissue scales. Computer models not only provide detailed insight into the interacting mechanisms of muscle adaptation; they can also serve as valuable tools to predict outcomes of pharmaceutical or interventional treatment, and help design individualized training, treatment, and rehabilitation plans.

Acknowledgments This work was supported by the National Science Foundation Graduate Research Fellowship and by the Stanford Graduate Engineering Fellowship to Katrina Wisdom, by the National Institutes of Health Grants R24 HD065690 and U54 GM072970 to Scott Delp, and by the National Science Foundation CAREER award CMMI 0952021 and INSPIRE grant 1233054 and by the National Institutes of Health Grant U01 HL119578 to Ellen Kuhl. Thank you to Dr Richard Lieber, Alexander Real, Aleksandra Denisin, and Alexander Zöllner for helpful conversations, and to David Delp for the illustrations.

References

Aagaard P, Andersen JL, Dyhre-Poulsen P, Leffers AM, Wagner A et al (2001) A mechanism for increased contractile strength of human pennate muscle in response to strength training: changes in muscle architecture. J Physiol 534:613–623

Adams GR, Caiozzo VJ, Baldwin KM (2003) Skeletal muscle unweighting: spaceflight and ground-based models. J Appl Physiol 95:2185–2201

Ahtikoski A, Koskinen SO, Virtanen P, Kovanen V, Takala TE (2001) Regulation of synthesis of fibrillar collagens in rat skeletal muscle during immobilization in shortened and lengthened positions. Acta Physiol Scand 172:131–140

Akeson W, Amiel D, Mechanic G, Woo S, Harwood F et al (1977) Cross-linking alterations in joint contractures: changes in the reducible cross-links in periarticular connective tissue collagen after nine weeks of immobilization. Connect Tissue Res 5:15–19

Akima H, Kubo K, Imai M, Kanehisa H, Suzuki Y et al (2001) Inactivity and muscle: effect of resistance training during bed rest on muscle size in the lower limb. Acta Physiol Scand 172:269–278

Allen D, Linderman J (1997) Growth hormone/IGF-I and/or resistive exercise maintains myonuclear number in hindlimb unweighted muscles. J Appl Physiol 83:1857–1861

Allen DL, Roy RR, Edgerton VR (1999) Myonuclear domains in muscle adaptation and disease. Muscle Nerve 22:1350–1360

Ambrosi D, Ateshian GA, Arruda EM, Cowin SC, Dumais J, Goriely A, Holzapfel GA, Humphrey JD, Kemkemer R, Kuhl E, Olberding JE, Taber LA, Garikipati K (2011) Perspectives on biological growth and remodeling. J Mech Phys Solids 59:863–883

Andersen J, Aagaard P (2000) Myosin heavy chain IIX overshoot in human skeletal muscle. Muscle Nerve 23:1095–1104

Arnold EM, Delp SL (2011) Fibre operating lengths of human lower limb muscles during walking. Phil Trans R Soc B 366:1530–1539

Asakawa DS, Pappas GP, Drace JE, Delp SL (2002) Aponeurosis length and fascicle insertion angles of the biceps brachii. J Mech Med Biol 2:449–455

Ausoni S, Gorza L, Schiaffino S, Gundersen K, Lomo T (1990) Expression of myosin heavy chain isoforms in stimulated fast and slow rat muscles. J Neurosci 10:153–160

Baker JH, Matsumoto DE (1988) Adaptation of skeletal muscle to immobilization in a shortened position. Muscle Nerve 11:231–244

Baldwin K, Haddad F (2001) Invited review: effects of different activity and inactivity paradigms on myosin heavy chain gene expression in striated muscle. J Appl Physiol 90:345–357

Bamman M, Clarke M (1998) Impact of resistance exercise during bed rest on skeletal muscle sarcopenia and myosin isoform distribution. J Appl Physiol 84:157–163

Berg H, Larsson L, Tesch P (1997) Lower limb skeletal muscle function after 6 wk of bed rest. J Appl Physiol 82:182–188

Berg HE, Eiken O, Miklavcic L, Mekjavic IB (2007) Hip, thigh and calf muscle atrophy and bone loss after 5-week bedrest inactivity. Eur J Appl Physiol 99:283–289

Billeter R, Puntschort A, Vogt M, Wittwer M, Wey E (1997) Molecular biology of human muscle adaptation. Int J Sports Med 18:S300–S301

Blazevich AJ, Cannavan D, Coleman DR, Horne S (2007) Influence of concentric and eccentric resistance training on architectural adaptation in human quadriceps muscles. J Appl Physiol 103:1565–1575

Blemker SS, Delp SL (2005) Three-dimensional representation of complex muscle architectures and geometries. Ann Biomed Eng 33:661–673

Blemker SS, Pinsky PM, Delp SL (2005) A 3D model of muscle reveals the causes of nonuniform strains in the biceps brachii. J Biomech 38:657–665

Blemker SS, Delp SL (2006) Rectus femurs and vast us intermedius fiber excursions predicted by three-dimensional muscle models. J Biomech 39:1383–1391

Boakes JL, Foran J, Ward SR, Lieber RL (2007) Muscle adaptation by serial sarcomere addition 1 year after femoral lengthening. Clin Orthop Relat Res 456:250–253

Böl M, Reese S (2008) Micromechanical modelling of skeletal muscles based on the finite element method. Comput Methods Biomech Biomed Eng 11:489–504

Böl M (2010) Micromechanical modelling of skeletal muscles: from the single fiber to the whole muscle. Arch Appl Mech 80:557–567

Böl M, Leichsenring K, Weichert C, Sturmat M, Schenk P, Blickhan R, Siebert T (2013) Three-dimensional surface geometries of the rabbit soleus muscle during contraction: input for biomechanical modeling and its validation. Biomech Model Mechanobiol 12:1205–1220

Booth FW, Thomason DB (1991) Molecular and cellular adaptation of muscle in response to exercise: perspectives of various models. Physiol Rev 71:541–585

Bottinelli R, Canepari M, Pellegrino M, Reggiani C (1996) Force-velocity properties of human skeletal muscle fibres: myosin heavy chain isoform and temperature dependence. J Physiol 495: 573–586

Brockett CL, Morgan DL, Proske U (2001) Human hamstring muscles adapt to eccentric exercise by changing optimum length. Med Sci Sports Exerc 33:783–790

Burkholder TJ, Fingado B, Baron S, Lieber RL (1994) Relationship between muscle fiber types and sizes and muscle architectural properties in the mouse hindlimb. J Morphol 221:177–90

Burkholder TJ, Lieber RL (1998) Sarcomere number adaptation after retinaculum transection in adult mice. J Exp Biol 201:309–316

Bustamante AC, Marko JF, Siggia ED, Smith S (1994) Entropic elasticity of lambda-phage DNA. Science 265:1599–1600

Caiozzo V, Haddad F, Baker M, Herrick R, Prietto N et al (1996) Microgravity-induced transformations of myosin isoforms and contractile properties of skeletal muscle. J Appl Physiol 81:123–132

Caiozzo V, Baker M, Baldwin K (1997) Modulation of myosin isoform expression by mechanical loading: role of stimulation frequency. J Appl Physiol 82:211–218

Caiozzo VJ, Utkan A, Chou R, Khalafi A, Chandra H et al (2002) Effects of distraction on muscle length: mechanisms involved in sarcomerogenesis. Clin Orthop Relat Res 403:S133–S145

Caiozzo V (2002) Plasticity of skeletal muscle phenotype: mechanical consequences. Muscle Nerve 26:740–768

Campbell EL, Seynnes OR, Bottinelli R, McPhee JS, Atherton PJ et al (2013) Skeletal muscle adaptations to physical inactivity and subsequent retraining in young men. Biogerontology 14:247–259

Canon F, Goubel F (1995) Changes in stiffness induced by hindlimb suspension in rat soleus muscle. Pflugers Arch 429:332–337

Carson JA, Wei L (2000) Integrin signaling's potential for mediating gene expression in hypertrophying skeletal muscle. J Appl Physiol 88:337–343

Cromie MJ, Sanchez GN, Schnitzer MJ, Delp SL (2013) Sarcomere lengths in human extensor carpi radials brevis measured by microendoscropy. Muscle Nerve 48:286–292

Csapo R, Maganaris CN, Seynnes OR, Narici MV (2010) On muscle, tendon and high heels. J Exp Biol 213:2582–2588

D'Antona G, Pellegrino MA, Adami R, Rossi R, Carlizzi CN et al (2003) The effect of ageing and immobilization on structure and function of human skeletal muscle fibres. J Physiol 552:499–511

D'Antona G, Lanfranconi F, Pellegrino MA, Brocca L, Adami R et al (2006) Skeletal muscle hypertrophy and structure and function of skeletal muscle fibres in male body builders. J Physiol 570:611–627

Dash RK, Dibella Ja, Cabrera ME (2007) A computational model of skeletal muscle metabolism linking cellular adaptations induced by altered loading states to metabolic responses during exercise. Biomed Eng Online 6:14

de Boer MD, Maganaris CN, Seynnes OR, Rennie MJ, Narici MV (2007) Time course of muscular, neural and tendinous adaptations to 23 day unilateral lower-limb suspension in young men. J Physiol 583:1079–1091

DeFreitas JM, Beck TW, Stock MS, Dillon MA, Kasishke PR (2011) An examination of the time course of training-induced skeletal muscle hypertrophy. Eur J Appl Physiol 111:2785–2790

Delp SL, Zajac FE (1992) Force- and moment-generating capacity of lower-extremity muscles before and after tendon lengthening. Clin Orthop Relat Res 284:247–259

Deschenes M (2001) A comparison of the effects of unloading in young adult and aged skeletal muscle. Med Sci Sports Exerc 33:1477–1483

Deschenes MR, Kraemer WJ (2002) Performance and physiologic adaptations to resistance training. Am J Phys Med Rehabil 81:S3–16

De Deyne PG, Hayatsu K, Meyer R, Paley D, Herzenberg JE (1999) Muscle regeneration and fiber-type transformation during distraction osteogenesis. J Orthop Res 17:560–570

De Deyne P (2002) Lengthening of muscle during distraction osteogenesis. Clin Orthop Relat Res 403S:S171–S177

Edgerton V, Zhou M, Ohira Y, Klitgaard H, Jiang B et al (1995) Human fiber size and enzymatic properties after 5 and 11 days of spaceflight. J Appl Physiol 78:1733–1739

Ehler E, Gautel M (2008) The sarcomere and sarcomerogenesis. In: Laing NG (ed) Sarcomere Skelet Muscle Disease. Landes Biosience and Springer+Business Media, pp 1–14

Elsalanty M, Makarov M, Cherkashin A, Birch J, Samchukov M (2007) Changes in pennate muscle architecture after gradual tibial lengthening in goats. Anat Rec 290:461–467

Eriksson A, Kadi F, Malm C, Thornell LE (2005) Skeletal muscle morphology in power-lifters with and without anabolic steroids. Histochem Cell Biol 124:167–175

Erskine RM, Jones DA, Williams AG, Stewart CE, Degens H (2010) Resistance training increases in vivo quadriceps femoris muscle specific tension in young men. Acta Physiol 199:83–89

Farup J, Kjølhede T, Sørensen H, Dalgas U, Møller AB et al (2012) Muscle morphological and strength adaptations to endurance vs. resistance training. J Strength Cond Res 26:398–407

Fitts RH, Trappe SW, Costill DL, Gallagher PM, Creer A et al (2010) Prolonged space flight-induced alterations in the structure and function of human skeletal muscle fibres. J Physiol 588:3567–3592

Fournier M, Roy R, Perham H, Simard C, Edgerton V (1983) Is limb immobilization a model of muscle disuse? Exp Neurol 80:147–156

Fowles J, MacDougall J, Tarnopolsky M, Sale D, Roy B et al (2000) The effects of acute passive stretch on muscle protein synthesis in humans. Can J Appl Physiol 25:165–180

Fry AC (2004) The role of resistance exercise intensity on muscle fibre adaptations. Sports Med 34:663–679

Gajdosik RL (2001) Passive extensibility of skeletal muscle: review of the literature with clinical implications. Clin Biomech 16:87–101

Gajdosik RL, Allred JD, Gabbert HL, Sonsteng BA (2007) A stretching program increases the dynamic passive length and passive resistive properties of the calf muscle-tendon unit of unconditioned younger women. Eur J Appl Physiol 99:449–454

Gautel M (2011) Cytoskeletal protein kinases: titin and its relations in mechanosensing. Pflugers Arch 462:119–134

Gibson JNA, Halliday D, Morrison WL, Stoward PJ, Hornsby GA et al (1987) Decrease in human quadriceps muscle protein turnover consequent upon leg immobilization. Clin Sci 72:503–509

Gillies AR, Lieber RL (2011) Structure and function of the skeletal muscle extracellular matrix. Muscle Nerve 44:318–331

Göktepe S, Abilez OJ, Kuhl E (2010) A generic approach towards finite growth with examples of athlete's heart, cardiac dilation, and cardiac wall thickening. J Mech Phys Solids 58:1661–1680

Göktepe S, Abilez OJ, Parker KK, Kuhl E (2010a) A multiscale model for eccentric and concentric cardiac growth through sarcomerogenesis. J Theor Biol 265:433–442

Goldspink D (1978) The influence of passive stretch on the growth and protein turnover of the denervated extensor digitorum longus muscle. Biochem J 174:595–602

Goldspink G, Scutt A (1992) Gene expression in skeletal muscle in response to stretch and force generation. Am J Physiol Integr Comp Physiol 262:R356–R363

Goldspink G (1999) Changes in muscle mass and phenotype and the expression of autocrine and systemic growth factors by muscle in response to stretch and overload. J Anat 194:323–334

Goldspink G, Yang SY (2001) Gene expression associated with muscle adaptation in response to physical signals. Cell Mol Response Stress 2:87–96

Gordon A, Huxley A, Julian F (1966) The variation in isometric tension with sarcomere length in vertebrate muscle fibres. J Physiol 184:170–192

Gossman MR, Sahrmann SA, Rose SJ (1982) Review of length-associated changes in muscle. Experimental evidence and clinical implications. Phys Ther 62:1799–1808

Goto K, Okuyama R, Honda M, Uchida H, Akema T et al (2003) Profiles of connecting (titin) in atrophied soleus muscle induced by unloading of rats. J Appl Physiol 94:897–902

Granzier H, Helmes M, Cazorla O, McNabb M, Labeit D et al (2000) Mechanical properties of titin isoforms. Elast Filam Cell 481:283–304

Gregory P, Low RB, Stirewalt WS (1986) Changes in skeletal-muscle myosin isoenzymes with hypertrophy and exercise. Biochem J 238:55–63

Grossman EJ, Roy RR, Talmadge RJ, Zhong H, Edgerton VR (1998) Effects of inactivity on myosin heavy chain composition and size of rat soleus fibers. Muscle Nerve 21:375–389

Gruther W, Benesch T, Zorn C, Paternostro-Sluga T, Quittan M et al (2008) Muscle wasting in intensive care patients: ultrasound observation of the M. quadriceps femoris muscle layer. J Rehabil Med 40:185–189

Hackney KJ, Ploutz-Snyder LL (2012) Unilateral lower limb suspension: integrative physiological knowledge from the past 20 years (1991–2011). Eur J Appl Physiol 112:9–22

Haddad F, Roy R (2003) Atrophy responses to muscle inactivity. II. Molecular markers of protein deficits. J Appl Physiol 95:791–802

Haddad F, Roy RR, Zhong H, Edgerton VR, Baldwin KM (2003) Atrophy responses to muscle inactivity. I. Cellular markers of protein deficits. J Appl Physiol 95:781–790

Hanson AM, Harrison BC, Young MH, Stodieck LS, Ferguson VL (2012) Longitudinal characterization of functional, morphologic, and biochemical adaptations in mouse skeletal muscle with hindlimb suspension. Muscle Nerve 48:393–402

Hedayatpour N, Falla D (2012) Non-uniform muscle adaptations to eccentric exercise and the implications for training and sport. J Electromyogr Kinesiol 22:329–333

Heslinga JW, te Kronnie G, Huijing PA (1995) Growth and immobilization effects on sarcomeres: a comparison between gastrocnemius and soleus muscles of the adult rat. Eur J Appl Physiol Occup Physiol 70:49–57

Hill AV (1938) The heat of shortening and dynamics constants of muscles. Proc R Soc Lond B 126:136–195

Hoang PD, Herbert RD, Gandevia SC (2007) Effects of eccentric exercise on passive mechanical properties of human gastrocnemius in vivo. Med Sci Sports Exerc 39:849–857

Holzapfel GA (2000) Nonlinear solid mechanics: a continuum approach for engineering John Wiley & Sons, Chichester. Q11

Holzapfel GA, Gasser TC, Ogden RW (2000) A new constitutive framework for anterial wall mechanics and a comparative study of material models. J Elast 61:1–48

Hubbard R, Ianuzzo C, Linduska J (1975) Compensatory adaptation of skeletal muscle composition to a long term functional overload. Growth 39:85–93

Huijing PA (1999) Muscle as a collagen fiber reinforced composite: a review of force transmission in muscle and whole limb. J Biomech 32:329–345

Huxley HE, Hanson J (1954) Changes in the cross-striations of muscle during contraction and stretch and their structural interpretation. Nature 173:973–976

Ianuzzo C, Gollnick P, Armstrong R (1976) Compensatory adaptations of skeletal muscle fiber types to a long-term functional overload. Life Sci 19:1517–1524

Janecki D, Jarocka E, Jaskólska A (2011) Muscle passive stiffness increases less after the second bout of eccentric exercise compared to the first bout. J Sci Med Sport 14:338–343

Johnson T, Klueber K (1991) Skeletal muscle following tonic overload: functional and structural analysis. Med Sci Sports Exerc 23:49–55

Joo ST, Kim GD, Hwang YH, Ryu YC (2013) Control of fresh meat quality through manipulation of muscle fiber characteristics. Meat Sci 95:828–836

Jürimäe J, Abernethy PJ, Blake K, McEniery MT (1996) Changes in the myosin heavy chain isoform profile of the triceps brachii muscle following 12 weeks of resistance training. Eur J Appl Physiol Occup Physiol 74:287–292

Kasper CE, Xun L (2000) Expression of titin in skeletal muscle varies with hind-limb unloading. Biol Res Nurs 2:107–115

Kawakami Y (1993) Muscle-fiber pennation angles are greater in hypertrophied than in normal muscles. J Appl Physiol 74: 2740–2744

Kawakami Y, Abe T, Kuno SY, Fukunaga T (1995) Training-induced changes in muscle architecture and specific tension. Eur J Appl Physiol Occup Physiol 72:37–43

Kho AL, Perera S, Alexandrovich A, Gautel M (2012) The sarcomeric cytoskeleton as a target for pharmacological intervention. Curr Opin Pharmacol 12:347–354

Kirby TJ, McCarthy JJ (2013) MicroRNAs in skeletal muscle biology and exercise adaptation. Free Radic Biol Med 64:95–105

Kjaer M (2004) Role of extracellular matrix in adaptation of tendon and skeletal muscle to mechanical loading. Physiol Rev 84:649–698

Komi PV, Karlsson J (1979) Physical performance, skeletal muscle enzyme activities, and fibre types in monozygous and dizygous twins of both sexes. Acta Physiol Scand Suppl 462:1

Kovanen V, Suominen H, Peltonen L (1987) Effects of aging and lifelong physical training on collagen in slow and fast skeletal muscle in rats. A morphometric and immuno-histochemical study. Cell Tissue Res 248:247–255

Kraemer WJ, Nindl BC, Ratamess NA, Gotshalk LA, Volek JS et al (2004) Changes in muscle hypertrophy in women with periodized resistance training. Med Sci Sport Exerc 36:697–708

Kraus W, Torgan C, Taylor D (1994) Skeletal muscle adaptation to chronic low-frequency motor nerve stimulation. Exerc Sport Sci Rev 22:313–360

Kubo K, Kanehisa H (2001) Influence of static stretching on viscoelastic properties of human tendon structures in vivo. J Appl Physiol 90:520–527

Kubo K, Ikebukuro T, Yata H (2010) Time course of changes in muscle and tendon properties during strength training and detraining. J Strength Cond Res 24:322–331

Kuhl E, Holzapfel GA (2007) A continuum model for remodeling in living structures. J Math Sci 42:8811–8823

Kuhl E (2014) Growing matter—a review of growth in living systems. J Mech Behav Biomed Mat 29:529–543

LaRoche DP, Connolly DAJ (2006) Effects of stretching on passive muscle tension and response to eccentric exercise. Am J Sports Med 34:1000–1007

Lee SJ, McPherron AC (2001) Regulation of muscle activity and muscle growth. Proc Natl Acad Sci 98:9306–9311

Lemos RR, Epstein M, Herzog W, Wyvill B (2004) A framework for structured modeling of skeletal muscle. Comput Methods Biomech Biomed Eng 7:305–317

Lieber RL (2009) Skeletal muscle structure, function, and plasticity: the physiological basis of rehabilitation. M—medicine series. Wolters Kluwer Health/Lippincott Williams & Wilkins, Philadelphia

Lieber R, Friden J (2000) Functional and clinical significance of skeletal muscle architecture. Muscle Nerve 23:1647–1666

Lindsey CA, Makarov MR, Shoemaker S, Birch JG, Buschang PH et al (2002) The effect of the amount of limb lengthening on skeletal muscle. Clin Orthop Relat Res 402:278–287

Llewellyn ME, Barretto RPJ, Delp SL, Schnitzer MJ (2008) Minimally invasive high-speed imaging of sarcomere contractile dynamics in mice and humans. Nature 454:784–788

Lynn R, Morgan D (1994) Decline running produces more sarcomeres in rat vastus intermedius muscle fibers than does incline running. J Appl Physiol 77:1439–1444

MacDougall J, Sale D, Elder G, Sutton J (1982) Physiology of elite powerlifters and bodybuilders. Eur J Appl Physiol Occup Physiol 48:117–126

Mackey A, Holm L, Reitelseder S, Pedersen TG, Doessing S et al (2011) Myogenic response of human skeletal muscle to 12 weeks of resistance training at light loading intensity. Scand J Med Sci Sports 21:773–782

Magid A, Law D (1985) Myofibrils bear most of the resting tension in frog skeletal muscle. Science 230:1280–1282

Magnusson SP, Narici MV, Maganaris CN, Kjaer M (2008) Human tendon behaviour and adaptation, in vivo. J Physiol 586:71–81

Makarov M, Birch J, Samchukov M (2009) The role of variable muscle adaptation to limb lengthening in the development of joint contractures: an experimental study in the goat. J Pediatr Orthop 29:175–181

Matano T, Tamai K, Kurokawa T (1994) Adaptation of skeletal muscle in limb lengthening: a light diffraction study on the sarcomere length in situ. J Orthop Res 12:193–196

Maxwell LC, Faulkner JA, Hyatt GJ (1974) Estimation of number of fibers in guinea pig skeletal muscles. J Appl Physiol 37:259–264

McDonagh MJN, Davies CTM (1984) Adaptive response of mammalian skeletal muscle to exercise with high loads. Eur J Appl Physiol 52:139–155

Millard M, Uchida T, Seth A, Delp SL (2013) Flexing computational muscle: modeling and simulation of musculotendon dynamics. J Biomech Eng 135:021005

Miller BF, Olesen JL, Hansen M, Døssing S, Crameri RM et al (2005) Coordinated collagen and muscle protein synthesis in human patella tendon and quadriceps muscle after exercise. J Physiol 567:1021–1033

Moore DR, Phillips SM, Babraj JA, Smith K, Rennie MJ (2005) Myofibrillar and collagen protein synthesis in human skeletal muscle in young men after maximal shortening and lengthening contractions. Am J Physiol Endocrinol Metab 288:E1153–E1159

Münster S, Jawerth LM, Ba Leslie, Weitz JI, Fabry B et al (2013) Strain history dependence of the nonlinear stress response of fibrin and collagen networks. Proc Natl Acad Sci 110:12197–202

Murtada SC, Arner A, Holzapfel GA (2012) Experiments and mechanochemical modeling of smooth muscle contraction: significance of filament overlap. J Theor Biol 297:176–186

Mutungi G, Ranatunga KW (1996) The viscous, viscoelastic and elastic characteristics of resting fast and slow mammalian (rat) muscle fibres. J Physiol 496:827–836

Nakamura M, Ikezoe T, Takeno Y, Ichihashi N (2012) Effects of a 4-week static stretch training program on passive stiffness of human gastrocnemius muscle-tendon unit in vivo. Eur J Appl Physiol 112:2749–2755

Narici MV, Maganaris CN (2007) Plasticity of the muscle-tendon complex with disuse and aging. Exerc Sport Sci Rev 35:126–134

Neagoe C, Opitz CA, Makarenko I, Linke WA (2003) Gigantic variety: expression patterns of titin isoforms in striated muscles and consequences for myofibrillar passive stiffness. J Muscle Res Cell Motil 24:175–189

Nordez A, Cornu C, McNair P (2006) Acute effects of static stretching on passive stiffness of the hamstring muscles calculated using different mathematical models. Clin Biomech 21:755–760

Nordez A, Casari P, Mariot JP, Cornu C (2009) Modeling of the passive mechanical properties of the musculo-articular complex: acute effects of cyclic and static stretching. J Biomech 42:767–773

Ogneva IV (2010) Transversal stiffness of fibers and desmin content in leg muscles of rats under gravitational unloading of various durations. J Appl Physiol 109:1702–1709

Oliveira Milani J, Matheus J, Gomide L, Volpon J, Shimano A (2008) Biomechanical effects of immobilization and rehabilitation on the skeletal muscle of trained and sedentary rats. Ann Biomed Eng 36:1641–1648

Oomens C, Maenhout M, van Oijen C, Drost M, Baaijens F (2003) Finite element modelling of contracting skeletal muscle. Philos Trans R Soc Lond B Biol Sci 358:1453–1460

Pansarasa O, Rinaldi C, Parente V, Miotti D, Capodaglio P et al (2009) Resistance training of long duration modulates force and unloaded shortening velocity of single muscle fibres of young women. J Electromyogr Kinesiol 19:e290–e300

Patel T, Lieber R (1996) Force transmission in skeletal muscle: from actomyosin to external tendons. Exerc Sport Sci Rev 25:321–363

Pattullo MC, Cotter MA, Cameron NE, Barry JA (1992) Effects of lengthened immobilization on functional and histochemical properties of rabbit tibialis anterior muscle. Exp Physiol 77:433–442

Peters D, Barash IA, Burdi M, Yuan PS, Mathew L et al (2003) Asynchronous functional, cellular and transcriptional changes after a bout of eccentric exercise in the rat. J Physiol 553:947–957

Pette D, Staron RS (2000) Myosin isoforms, muscle fiber types, and transitions. Microsc Res Tech 50:500–509

Pontén E, Fridén J (2008) Immobilization of the rabbit tibialis anterior muscle in a lengthened position causes addition of sarcomeres in series and extra-cellular matrix proliferation. J Biomech 41:1801–1804

Potier TG, Alexander CM, Seynnes OR (2009) Effects of eccentric strength training on biceps femoris muscle architecture and knee joint range of movement. Eur J Appl Physiol 105:939–944

Prado LG, Makarenko I, Andresen C, Krüger M, Opitz C et al (2005) Isoform diversity of giant proteins in relation to passive and active contractile properties of rabbit skeletal muscles. J Gen Physiol 126:461–480

Psatha M, Wu Z, Gammie FM, Ratkevicius A, Wackerhage H et al (2012) A longitudinal MRI study of muscle atrophy during lower leg immobilization following ankle fracture. J Magn Reson Imaging 35:686–695

Purslow PP, Trotter JA (1994) The morphology and mechanical properties of endomysium in series-fibred muscles: variations with muscle length. J Muscle Res Cell Motil 15:299–308

Rausch MK, Dam A, Göktepe S, Abilez OJ, Kuhl E (2011) Computational modeling of growth: systemic and pulmonary hypertension in the heart. Biomech Model Mechanobiol 10:799–811

Reeves ND, Maganaris CN, Longo S, Narici MV (2009) Differential adaptations to eccentric versus conventional resistance training in older humans. Exp Physiol 94:825–833

Reid DA, Mcnair PJ (2004) Passive Force, Angle, and Stiffness Changes after Stretching of Hamstring Muscles. Med Sci Sport Exerc 36:1944–1948

Ricoy JR, Encinas AR, Cabello A, Madero S, Arenas J (1998) Histochemical study of the vastus lateralis muscle fibre types of athletes. J Physiol Biochem 54:41

Röhrle O, Davidson J, Pullan A (2008) Bridging scales: a three-dimensional electromechanical finite element model of skeletal muscle. SIAM J Sci Comput 30:2882–2904

Röhrle O (2010) Simulating the electro-mechanical behavior of skeletal muscles. Comput Sci Eng 12:48–58

Röhrle O, Davidson JB, Pullan A (2012) A physiologically based, multi-scale model of skeletal muscle structure and function. Front Physiol 3:1–14

Roig M, O'Brien K, Kirk G, Murray R, McKinnon P et al (2009) The effects of eccentric versus concentric resistance training on muscle strength and mass in healthy adults: a systematic review with meta-analysis. Br J Sports Med 43:556–568

Roy RR, Baldwin KM, Edgerton VR (1991) The plasticity of skeletal muscle: effects of neuromuscular activity. Exerc Sport Sci Rev 19:269–312

Saez P, Pena E, Martinez MA, Kuhl E (2013) Mathematical modeling of collagen turnover in biological tissue. J Math Biol 67:1765–1793

Sandler H (1986) Inactivity: physiological effects. Access Online via Elsevier

Schenk P, Siebert T, Hiepe P, Güllmar D, Reichenbach JR, Wick C, Blickhan R, Böl M (2013) Determination of three-dimensional muscle architectures: validation of the DTI-based fiber tractgraphy method by manual digitization. J Anatomy 223: 61–68

Scott W, Stevens J, BinderMacleod S (2001) Human skeletal muscle fiber type classifications. Phys Ther 81:1810–1816

Seger JY, Arvidsson B, Thorstensson A (1998) Specific effects of eccentric and concentric training on muscle strength and morphology in humans. Eur J Appl Physiol Occup Physiol 79:49–57

Seynnes OR, de Boer M, Narici MV (2007) Early skeletal muscle hypertrophy and architectural changes in response to high-intensity resistance training. J Appl Physiol 102:368–373

Seynnes OR, Maganaris CN, de Boer MD, di Prampero PE, Narici MV (2008) Early structural adaptations to unloading in the human calf muscles. Acta Physiol 193:265–274

Shah SB, Su FC, Jordan K, Milner DJ, Fridén J et al (2002) Evidence for increased myofibrillar mobility in desmin-null mouse skeletal muscle. J Exp Biol 205:321–325

Sherwood L (2010) Human physiology: from cells to systems Cengage Learning, Belmont, USA.

Shoepe TC, Stelzer JE, Garner DP, Widrick JJ (2003) Functional adaptability of muscle fibers to long-term resistance exercise. Med Sci Sports Exerc 35:944–951

Simoneau JA, Lortie G, Boulay MR, Marcotte M, Thibault MC et al (1985) Human skeletal muscle fiber type alteration with high-intensity intermittent training. Eur J Appl Physiol Occup Physiol 54:250–253

Simpson A, Williams P (1995) The response of muscle to leg lengthening. J Bone Joint Surg 77:630–636

Smith LR, Lee KS, Ward SR, Chambers HG, Lieber RL (2011) Hamstring contractures in children with spastic cerebral palsy result from a stiffer extracellular matrix and increased in vivo sarcomere length. J Physiol 589:2625–2639

Storm C, Pastore JJ, MacKintosh FC, Lubensky TC, Janmey PA (2005) Nonlinear elasticity in biological gels. Nature 435:191–194

Tabary J, Tabary C, Tardieu C (1972) Physiological and structural changes in the cat's soleus muscle due to immobilization at different lengths by plaster casts. J Physiol 224:231–244

Taber LA (1995) Biomechanics of growth, remodeling, and morphogenesis. Appl Mech Rev 48:487–545

Taber LA (1998) Biomechanical growth laws for muscle tissue. J Theor Biol 193:201–213

Talmadge R, Roy R (1996) MHC and sarcoplasmic reticulum protein isoforms in functionally overloaded cat plantaris muscle fibers. J Appl Physiol 80:1296–1303

Tardieu C, Tabary JC, Tabary C, Tardieu G (1982) Adaptation of connective tissue length to immobilization in the lengthened and shortened positions in cat soleus muscle. J Physiol 78:214–220

Tesch P (1988) Skeletal muscle adaptations consequent to long-term heavy resistance exercise. Med Sci Sports Exerc 20:S132–S134

Thelen DG (2003) Adjustment of muscle mechanics model parameters to simulate dynamic contractions in older adults. J Biomech Eng 125:70–77

Thomason D, Booth F (1990) Atrophy of the soleus muscle by hindlimb unweighting. J Appl Physiol 68:1–12

Tidball JG (2005) Mechanical signal transduction in skeletal muscle growth and adaptation. J Appl Physiol 98:1900–1908

Toursel T, Stevens L, Granzier H, Mounier Y (2002) Passive tension of rat skeletal soleus muscle fibers: effects of unloading conditions. J Appl Physiol 92:1465–1472

Trappe S (2002) Effects of spaceflight, simulated spaceflight and countermeasures on single muscle fiber physiology. J Gravit Physiol 9:P323–P326

Trappe S, Trappe T, Gallagher P, Harber M, Alkner B et al (2004) Human single muscle fibre function with 84 day bed-rest and resistance exercise. J Physiol 557:501–513

Tskhovrebova L, Trinick J, Sleep JA, Simmons R (1997) Elasticity and unfolding of single molecules of the giant muscle protein titin. Nature 387:308–312

Wang K, Ramirez-Mitchell R (1983) A network of transverse and longitudinal intermediate filaments is associated with sarcomeres of adult vertebrate skeletal muscle. J Cell Biol 96:562–570

Wickiewicz T, Roy R (1983) Muscle architecture of the human lower limb. Clin Orthop Relat Res 179:275–283

Widrick J, Romatowski J, Bain J, Trappe S, Trappe T et al (1997) Effect of 17 days of bed rest on peak isometric force and unloaded shortening velocity of human soleus fibers. Am J Physiol Physiol 273:C1690–C1699

Widrick JJ, Knuth ST, Norenberg KM, Romatowski JG, Bain JL et al (1999) Effect of a 17 day spaceflight on contractile properties of human soleus muscle fibres. J Physiol 516:915–930

Widrick JJ, Trappe SW, Romatowski JG, Da Riley, Costill DL et al (2002) Unilateral lower limb suspension does not mimic bed rest or spaceflight effects on human muscle fiber function. J Appl Physiol 93:354–360

Williams PE, Goldspink G (1971) Longitudinal growth of striated muscle fibres. J Cell Sci 9:751–767

Williams PE, Goldspink G (1973) The effect of immobilization on the longitudinal growth of striated muscle fibres. J Anat 116:45–55

Williams PE, Goldspink G (1978) Changes in sarcomere length and physiological properties in immobilized muscle. J Anat 127:459–468

Williams P, Goldspink G (1984) Connective tissue changes in immobilised muscle. J Anat 138:343–350

Williams P, Catanese T (1988) The importance of stretch and contractile activity in the prevention of connective tissue accumulation in muscle. J Anat 158:109–114

Williams P, Kyberd P, Simpson H, Kenwright J, Goldspink G (1998) The morphological basis of increased stiffness of rabbit tibialis anterior muscles during surgical limb lengthening. J Anat 193:131–138

Williamson D (2001) Reduction in hybrid single muscle fiber proportions with resistance training in humans. J Appl Physiol 91:1955–1961

Woo S, Matthews J, Akeson W, Amiel D, Convery F (1975) Connective tissue response to immobility. Arthritis Rheum 18:257–264

Wren T (2003) A computational model for the adaptation of muscle and tendon length to average muscle length and minimum tendon strain. J Biomech 36:1117–1124

Yasuda N, Glover EI, Phillips SM, Isfort RJ, Tarnopolsky MA (2005) Sex-based differences in skeletal muscle function and morphology with short-term limb immobilization. J Appl Physiol 99:1085–1092

Ye F, Baligand C, Keener JE, Vohra R, Lim W et al (2013) Hindlimb muscle morphology and function in a new atrophy model combining spinal cord injury and cast immobilization. J Neurotrauma 30:227–235

Yokogawa M, Yamazaki T, Inoue K, Inaoka P, Tsuji K et al (2008) Age-associated changes in atrophy of the extensor digitorum longus muscle in hindlimb-suspended rats. J Phys Ther Sci 20:129–133

Yu JG, Carlsson L, Thornell LE (2004) Evidence for myofibril remodeling as opposed to myofibril damage in human muscles with DOMS: an ultrastructural and immunoelectron microscopic study. Histochem Cell Biol 121:219–227

Yucesoy CA, Koopman BHFJM, Baan GC, Grootenboer HJ, Huijing PA (2003) Effects of inter- and extramuscular myofascial force transmission on adjacent synergistic muscles: assessment by experiments and finite-element modeling. J Biomech 36:1797–1811

Zhou M, Klitgaard H, Saltin B, Roy R, Edgerton V et al (1995) Myosin heavy chain isoforms of human muscle after short-term spaceflight. J Appl Physiol 78:1740–1744

Zöllner AM, Abilez O, Böl M, Kuhl E (2012) Stretching skeletal muscle: chronic muscle lengthening through sarcomerogenesis. PLoS One 7:e45661